Supporting Information

Iridium(I) Complexes Bearing Hemilabile Coumarin-Functionalised N-Heterocyclic Carbene Ligands with Application as Alkyne Hydrosilylation Catalysts

Mert Olgun Karataş,[a,b,c] Bülent Alıcı,[b,c] Vincenzo Passarelli,[a] Ismail Özdemir,[b,c] Jesús J. Pérez-Torrente,*[a] and Ricardo Castarlenas,*[a]

[a]Departamento de Química Inorgánica – Instituto de Síntesis Química y Catálisis Homogénea (ISQCH), Universidad de Zaragoza – CSIC, C/ Pedro Cerbuna 12, 50009 Zaragoza, Spain

[b]Department of Chemistry, Faculty of Sciences, Inonu University, 44280, Malatya, Turkey

[c]Catalysis Reseach and Application Center, İnönü University, 44280 Malatya (Turkey)

E-mail: rcastar@unizar.es, perez@unizar.es

Table of contents

1. Synthesis of (4-chloromethylene)coumarin derivatives (1a-c)

1a-c were prepared according to the procedure described by Frasinyuk *et al*.[1] Compound **1a** was available from our previous study.[2]

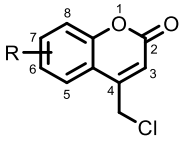

1a, R: 7,8-Me_2; **1b**, R: 6,7-Me_2; **1c**, R: 6-OMe

Chart S1. (4-chloromethylene)coumarin derivatives used in this study.

Chloromethylene-6,7-dimethyl-2*H*-chromene-2-one (1b). White solid, (69%), mp: 216-218 ^{o}C (lit. 215-217 ^{o}C).[1] IR (cm^{-1}): 1717 (C=O), 1638 (C=C). ^{1}H NMR (300 MHz, DMSO-d_6, 298 K): δ 7.62 (s, 1H, H_{Ar}), 7.27 (s, 1H, H_{Ar}), 6.59 (s, 1H, C=C<u>H</u>), 5.00 (s, 2H, C<u>H_2</u>Cl), 2.33 and 2.31 both (s, 6H, $H_{ArC\underline{H}3}$). ^{13}C NMR (75 MHz, DMSO-d_6, 298 K): δ 159.9 (C=O), 151.7, 150.7, 142.3, 132.9, 125.0, 117.1, 114.6, 114.2, 41.2, 19.6, 18.9.

4-Chloromethylene-6-methoxy-2*H*-chromene-2-one (1c). Green solid, (49%), mp: 122-123 ^{o}C. IR (cm^{-1}): 1718 (C=O), 1622 (C=C). ^{1}H NMR (300 MHz, DMSO-d_6, 298 K): δ 7.41 (m, 1H, H_{Ar}), 7.32 (m, 1H, H_{Ar}), 7.27 (m, 1H, H_{Ar}), 6.69 (s, 1H, C=C<u>H</u>), 5.07 (s, 2H, C<u>H_2</u>Cl), 3.85 (s, 3H, $H_{ArOC\underline{H}3}$). ^{13}C NMR (75 MHz, DMSO-d_6, 298 K): δ 160.2 (C=O), 156.0, 150.9, 148.1, 119.9, 118.3, 118.0, 116.2, 108.7, 56.3, 41.8.

2. Synthesis of imidazolium and benzimidazolium chlorides (2a-e and 3a-c)

Coumarin-functionalized imidazolium and benzimidazolium salts, **2a**-**b** and **3b**-**c**, respectively, were prepared according to the procedure described by us for the synthesis of **2c-e** and **3a.**[2]

General method. A DMF solution (5 mL) of **1** (5 mmol) and the corresponding *N*-alkylimidazole or *N*-alkylbenzimidazole (5 mmol) was heated for 3 days at 363 K. The mixture was allowed to cool to room temperature and then acetone (20 mL) was added to give a white precipitate which was collected by filtration. The crude product was washed with acetone (2 x 10 mL) and diethyl ether (2x10 mL), and dried under reduced pressure to afford the salts as white solids. Chemical shifts (expressed in parts per million) are referenced to residual solvent peaks (^{1}H, ^{13}C{1H}). Coupling constants, *J*, are given in Hz. Spectral assignments were achieved by combination of ^{1}H-^{1}H COSY, ^{13}C{^{1}H}-APT and ^{1}H-^{13}C HSQC/HMBC experiments.

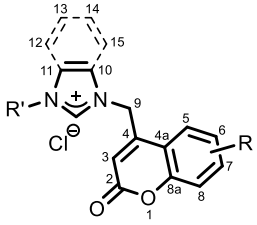

Imidazolium salts

2a (R=7,8-$(CH_3)_2$, R'= -CH_3)
2b (R=6-OCH_3, R'=-CH_3)
2c (R=7,8-$(CH_3)_2$, R'=-$CH=CH_2$)
2d (R=7,8-$(CH_3)_2$, R'=-$(CH_2)_3CH_3$)
2e (R=7,8-$(CH_3)_2$, R'=-$CH_2C_6H_5$)

Benzimidazolium salts

3a (R=-7,8-$(CH_3)_2$, R'=-$CH_2C_6H_4$-4-CH_3)
3b (R=-6,7-$(CH_3)_2$, R'=-$CH_2C_6H_4$-4-CH_3)
3c (R=-6,7-$(CH_3)_2$, R'=-$(CH_2)_3CH_3$)

Chart S2. Coumarin-functionalized carbene precursors used in this study.

1-Methyl-3-((7,8-dimethyl-2*H*-chromene-2-one-4-yl)methyl)imidazolium chloride (2a). White solid, 1.1 g (72%). IR (cm^{-1}): 1710 (C=O), 1629 (C=C), 1606 (C=N). ^{1}H NMR (300 MHz, DMSO-d_6, 298 K): δ 9.48 (s, 1H, NC<u>H</u>N), 7.94 and 7.86 (both m, 2H, H_{10} and H_{11}), 7.63 (d, $J_{H\text{-}H}$= 8.1 Hz, 1H, H_5), 7.26 (d, $J_{H\text{-}H}$= 8.1 Hz, H_6), 6.07 (s, 1H, H_3), 5.89 (s, 2H, H_9), 3.91 (s, 3H, NC<u>H</u>$_3$), 2.38 (s, 3H, $H_{ArCH3\text{-}at\text{-}7\text{-}pos.}$), 2.29 (s, 3H, $H_{ArCH3\text{-}at\text{-}8\text{-}pos.}$). $^{13}C\{^{1}H\}$-APT NMR (75 MHz, DMSO-d_6, 298 K): δ 160.0 (C=O), 151.6 (C_{8a}), 150.0 (C_4), 142.7 (C_7), 138.3 (NCHN), 126.3 (C_6), 124.7 and 123.5 (C_{10} and C_{11}), 124.5 (C_8), 121.8 (C_5), 115.0 (C_{4a}), 113.6 (C_3), 48.8 (C_9), 36.6 (-NCH_3), 20.4 (ArCH_3-at-7-pos.), 11.7 (ArCH_3-at-8-pos.).

1-Methyl-3-((6-methoxy-2*H*-chromene-2-one-4-yl)methyl)imidazolium chloride (2b). White solid, 0.90 g (59%). IR (cm^{-1}): 1708 (C=O), 1626 (C=C), 1573 (C=N). ^{1}H NMR (300 MHz, DMSO-d_6, 298 K): δ 9.53 (s, 1H, NC<u>H</u>N), 7.98 and 7.88 (both m, 2H, H_{10} and H_{11}), 7.43, 7.37 and 7.29 (all m, 3H, H_5, H_7 and H_8), 6.16 (s, 1H, H_3), 5.98 (s, 2H, H_9), 3.93 (s, 3H, NC<u>H</u>$_3$), 3.87 (s, 3H, ArOC<u>H</u>$_3$). $^{13}C\{^{1}H\}$-APT NMR (75 MHz, DMSO-d_6, 298 K): δ 160.0 (C=O), 156.3 (C_6), 149.5 (C_4), 147.8 (C_{8a}), 138.3 (NCHN), 124.7 and 123.4 (C_{10} and C_{11}), 120.3, 118.4 and 108.1 (C_5, C_7 and C_8), 117.8 (C_{4a}), 114.8 (C_3), 56.6 (ArOCH_3), 48.8 (C_9), 36.6 (-NCH_3).

1-(4-Methylbenzyl)-3-(6,7-dimethyl-2*H*-chromene-2-one-4-yl)methyl)benzimidazolium chloride (3b). White solid, 1.85 g (83%). IR (cm^{-1}): 1732 (C=O), 1609 (C=C), 1562 (C=N). ^{1}H NMR (300 MHz, DMSO-d_6, 298 K): δ 10.18 (s, 1H, NCHN), 8.04 (m, 2H, H_{12} and H_{15}), 7.70 (s, 1H, H_5), 7.68 (m, 2H, H_{13} and H_{14}), 7.48 (d, $J_{H\text{-}H}$= 8.0 Hz, 2H, $H_{o\text{-}tol.}$), 7.32 (s, 1H, H_8), 7.24 (d, 2H, $J_{H\text{-}H}$=8.0 Hz, $H_{m\text{-}tol.}$), 6.21 (s, 2H, H_9), 5.96 (s, 1H, H_3), 5.78 (s, 2H, NC<u>H</u>$_2$Ph), 2.36 and 2.34 (both s, 6H, HArC<u>H</u>$_3$), 2.30 (s, 3H, C<u>H</u>$_{3tol}$). $^{13}C\{^{1}H\}$ NMR (75 MHz, DMSO-d_6, 298 K): δ 159.6 (C=O), 151.4 (C_{8a}), 148.5 (C_4), 143.5 (NCHN), 142.7 (C_7), 138.3 ($C_{q,p\text{-}tol.}$), 133.2 and 131.4 (C_{10} and C_{11}), 131.1 (C_6), 130.6 (NCH_2C_q), 129.5 ($C_{m\text{-}tol.}$), 128.6 ($C_{o\text{-}tol.}$), 127.1 and 126.9 (C_{13} and C_{14}), 124.5 (C_8), 117.2 (C_5), 114.5 (C_{4a}), 114.2 and 113.9 (C_{12} and C_{15}), 111.9 (C_3), 50.1 (NCH_2Ph), 46.5 (C_9), 20.7 (Ar$CH_{3\text{-}tol.}$), 19.7 (Ar$CH_{3\text{-}coumarin\text{-}7\text{-}pos.}$), 18.9 (Ar$CH_{3\text{-}coumarin\text{-}6\text{-}pos.}$).

1-Butyl-3-((6,7-dimethyl-2*H*-chromene-2-one-4-yl)methyl)benzimidazolium chloride (3c). White solid, 1.70 g (85%). IR (cm^{-1}): 1726 (-C=O), 1609 (-C=C-), 1566 (-C=N-). ^{1}H NMR (300 MHz, DMSO-d_6, 298 K): δ 10.32 (s, 1H, NCHN), 8.21 and 8.05 (both m, 2H, H_{12} and H_{15}), 7.75 (s, 1H, H_5), 7.72 (m, 2H, H_{13} and H_{14}), 7.32 (s, 1H, H_8), 6.25 (s, 2H, H_9), 5.96 (s, 1H, H_3), 4.57 (t, $J_{H\text{-}H}$= 7.2 Hz, 2H, NC<u>H</u>$_2$$CH_2$), 2.36 and 2.34 (both s, 6H, ArCH_3), 1.96 (m, 2H, NCH_2C<u>H</u>$_2$), 1.39 (m, 2H, C<u>H</u>$_2$$CH_3$), 0.95 (t, $J_{H\text{-}H}$= 7.3 Hz, 3H, CH_2C<u>H</u>$_3$). $^{13}C\{^{1}H\}$ NMR (75 MHz, DMSO-d_6, 298 K): δ 159.6 (C=O), 151.4 (C_{8a}), 148.5 (C_4), 143.4 (NCHN), 142.6 (C_7), 133.2 and 131.4 (C_{10} and C_{11}), 131.2 (C_6), 126.9 and 126.8 (C_{13} and C_{14}), 124.8 (C_8), 117.1 (C_5), 114.5 (C_{4a}), 114.0 and 113.8 (C_{12} and C_{15}), 111.9 (C_3), 46.8 (C_9), 46.4 (NCH_2), 30.3 (NCH_2<u>C</u>H_2), 19.7 (Ar$CH_{3\text{-}coumarin\text{-}7\text{-}pos.}$), 19.1 (<u>C</u>$H_2CH_3$), 18.8 (Ar$CH_{3\text{-}coumarim\text{-}6\text{-}pos.}$), 13.4 ($CH_2$<u>C</u>$H_3$).

3. Calculation of thermodynamic parameters

The thermodynamic parameters of the equilibria **TBPY-5 ⇆ SP-4** for **4a**, **4e** and **5b** (Scheme S1) were obtained analysing the dependence of the ^{1}H chemical shift of the H-3 hydrogen atom of the pyrone moiety in **4a**, **4e** and **5b** on the temperature (Table S1).

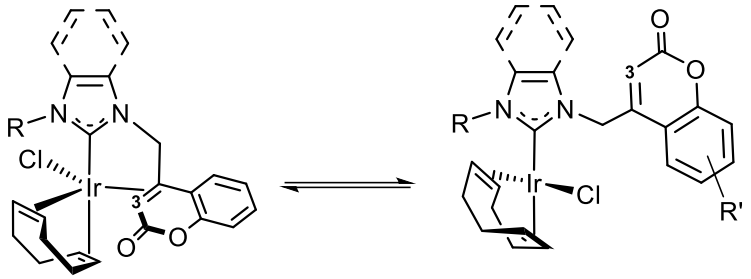

TBPY-5
4a, 4e, 5b

SP-4
4a', 4e', 5b'

4a, imidazolin, R = Me, R' = 7,8-Me_2
4e, imidazolin, R = benzyl, R' = 7,8- Me_2
5b, benzimidazolin, R = benzyl-4-Me, R' = 6,7-Me_2

Scheme S1. Equilibrium **TBPY-5 ⇆ SP-4** for **4a**, **4e**, and **5b**.

Table S1. ^{1}H chemical shifts (δ_{obs}) of the H-3 hydrogen atom of the pyrone moiety vs. temperature for **4a**, **4e** and **5b** in $CDCl_3$.

T (K)	δ_{obs} (4a)	δ_{obs} (4e)	δ_{obs} (5b)
213	3.41	3.52	3.75
303	4.65	5.17	5.17
313	4.87	5.39	5.32
323	5.05	5.5	5.45
333	5.21	5.61	5.54
343	5.38	5.7	5.61
353	-	-	5.66

Given the equilibrium **TBPY-5 ⇆ SP-4** depicted in Scheme S1, the equilibrium constant K_{eq} is

$$K_{eq} = \frac{[\boldsymbol{TBPY-5}]}{[\boldsymbol{SP-4}]} = \frac{\chi_{\boldsymbol{TBPY-5}}}{\chi_{\boldsymbol{SP-4}}}$$

Provided that above 283 K the equilibrium is in fast exchange regime, the observed chemical shift δ_{obs} of the H-3 hydrogen atom of the pyrone moiety at temperature higher than 283 K is:

$$\delta_{obs} = \chi_{\boldsymbol{TBPY-5}} \cdot \delta_{\boldsymbol{TBPY-5}} + \chi_{\boldsymbol{SP-4}} \cdot \delta_{\boldsymbol{SP-4}} \quad (a)$$

where $\delta_{\boldsymbol{TBPY-5}}$ and $\delta_{\boldsymbol{SP-4}}$ are the ^{1}H chemical shift of the hydrogen atom H-3 of the pyrone moiety in the **TBPY-5** and the **SP-4** species, respectively. $\delta_{\boldsymbol{TBPY-5}}$ is straightforwardly observed in the ^{1}H NMR spectrum at 213 K of **4a** (3.41 ppm), **4e** (3.52 ppm), and **5b** (3.75 ppm), where the equilibrium is in slow exchange regime and only the pentacoordinated isomer **TBPY–5** is detected. On the contrary, $\delta_{\boldsymbol{SP-4}}$ was obtained as a result of the fitting analysis (*vide infra*).

Thus, δ_{obs} can be expressed as a function of K_{eq}:

$$\delta_{obs} = \chi_{TBPY-5} \cdot \delta_{TBPY-5} + \chi_{SP-4} \cdot \delta_{SP-4} = \frac{1}{1 + K_{eq}} \cdot \left(\delta_{TBPY-5} + K_{eq} \cdot \delta_{SP-4}\right) \qquad (b)$$

and eventually as a function of ΔH_r and ΔS_r.

$$\delta_{obs} = \frac{1}{1 + e^{\left(-\frac{\Delta H_r}{RT} + \frac{\Delta S_r}{R}\right)}} \cdot \left(\delta_{TBPY-5} + \delta_{SP-4} \cdot e^{\left(-\frac{\Delta H_r}{RT} + \frac{\Delta S_r}{R}\right)}\right) \qquad (c)$$

Figure S1 shows the plot δ_{obs} vs. T for **4a**, **4e**, and **5b** and the fitting curves (equation *c*) along with the calculated parameters ΔH_r, ΔS_r and δ_{SP-4}, taking δ_{TBPY-5} = 3.75 ppm (**5b**), 3.41 (**4a**), 3.52 (**4e**) ppm (*cf.* Table S1).

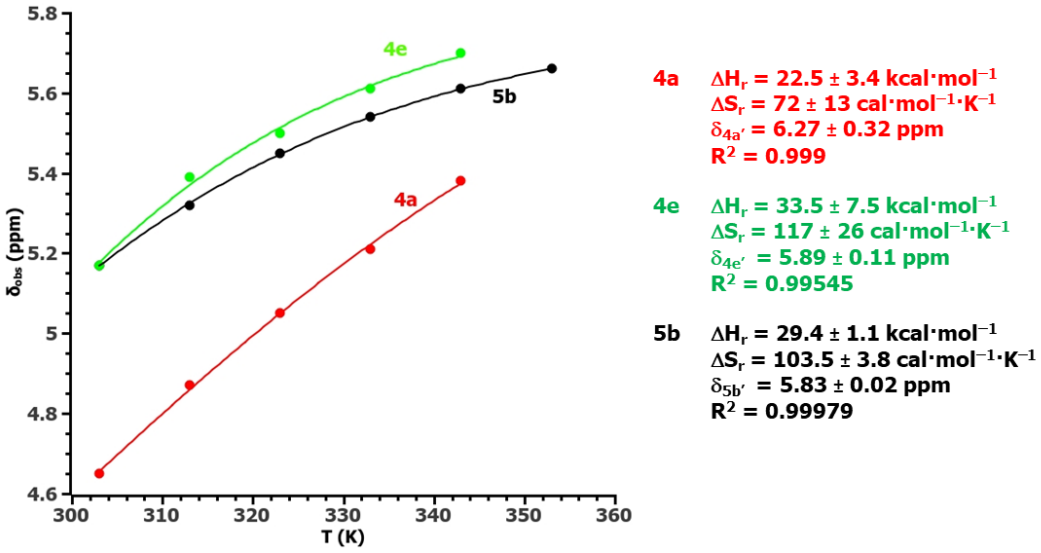

Figure S1. Scatter plot of the ^{1}H chemical shifts (δ_{obs}) of the H-3 hydrogen atom of the pyrone moiety vs. temperature for **4a** (red), **4e** (green) and **5b** (black) along with the fitted curves according to equation *c* (*vide infra*).

For the sake of comparison, Table S2 shows the calculated K_{eq} in the range 213-353 K along with the calculated molar fraction of the **TBPY–5** and **SP–4** isomers for **4a**, **4e**, and **5b**. Remarkably, in all the cases, at 213 K the **TBPY–5** isomer is almost the only species present in solution ($\chi_{TBPY-5} \geq 0.98$) whereas at 343 K the **SP–4** isomer is the major species.

Table S2. Calculated K_{eq}, χ_{TBPY-5} and χ_{SP-4} for the equilibrium **TBPY-5** ⇆ **SP-4** at different temperatures.

	4a			**4e**			**5b**		
T (K)	K_{eq}	χ_{TBPY-5}	χ_{SP-4}	K_{eq}	χ_{TBPY-5}	χ_{SP-4}	K_{eq}	χ_{TBPY-5}	χ_{SP-4}
213	0.018	0.98	0.02	0.008	0.99	0.01	0.016	0.98	0.02
243	0.084	0.92	0.08	0.081	0.92	0.08	0.122	0.89	0.11
293	0.562	0.64	0.36	1.38	0.42	0.58	1.46	0.41	0.59
333	1.704	0.37	0.63	7.19	0.12	0.88	6.23	0.14	0.86
353	2.701	0.27	0.73	14.3	0.07	0.93	11.4	0.08	0.92

4. Variable-temperature NMR spectra

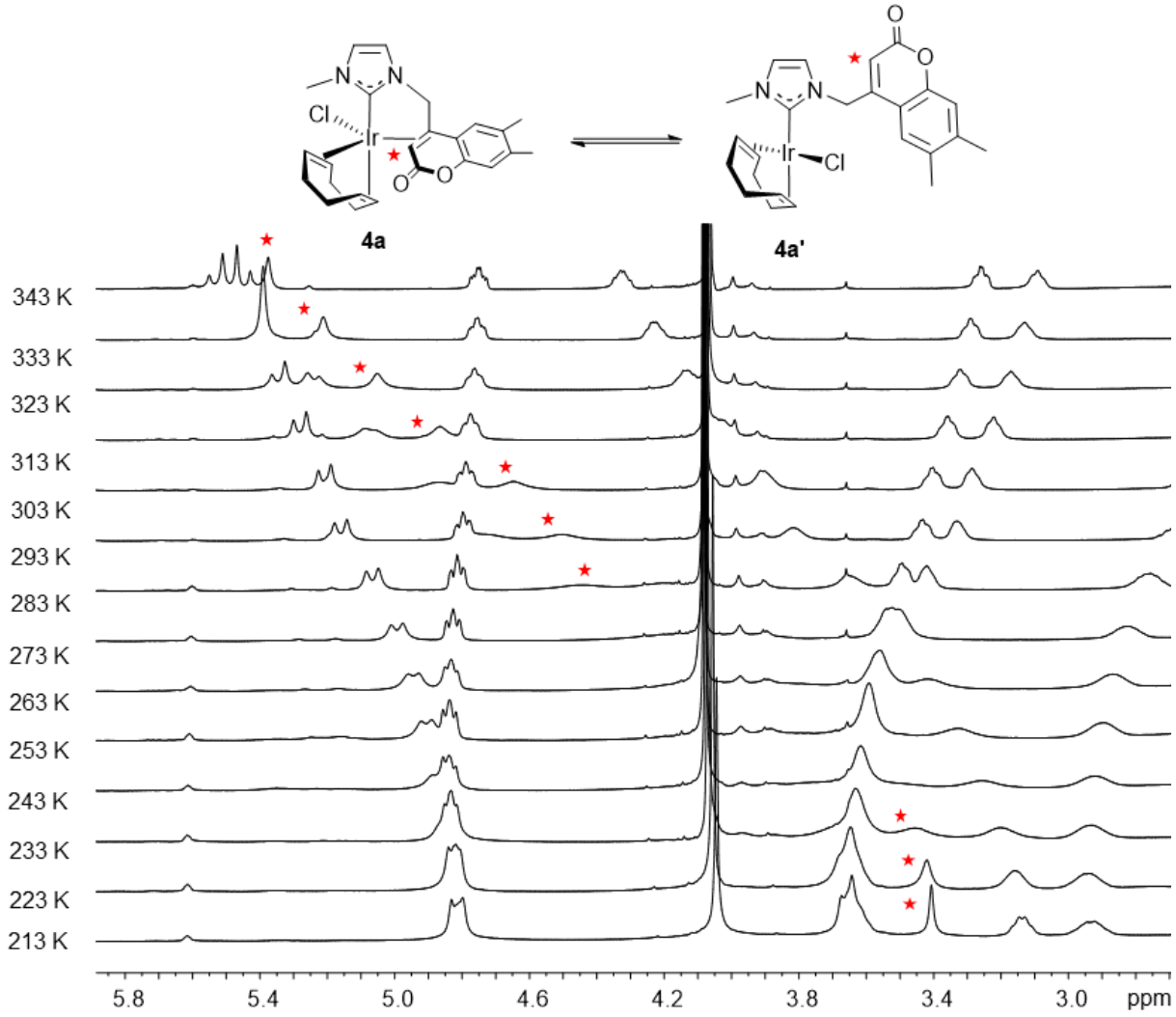

Figure S2. Stacked ^{1}H NMR spectra of **4a⇌4a'** in $CDCl_3$ at different temperatures.

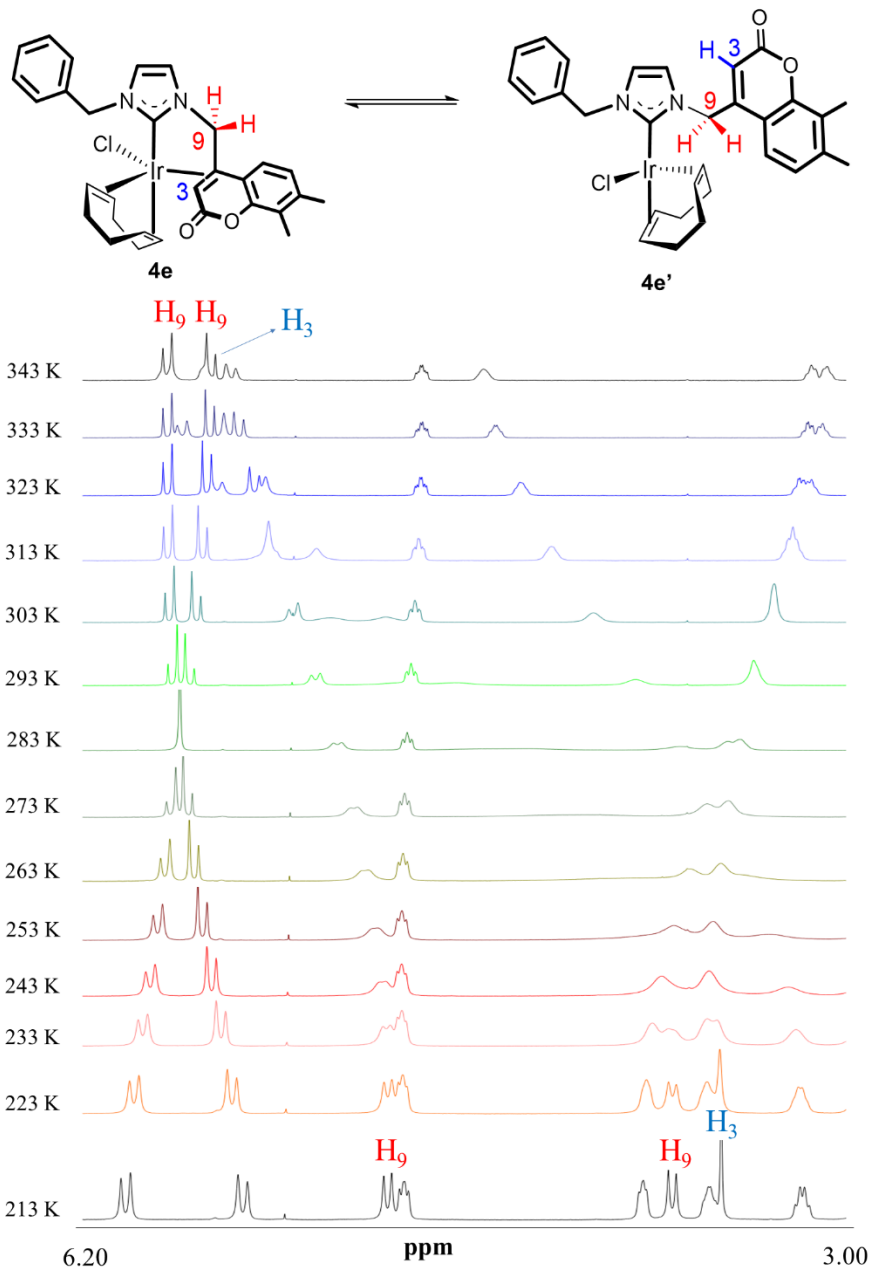

Figure S3. Staked ^{1}H NMR spectra of **4e⇌4e'** in $CDCl_3$ at different temperatures.

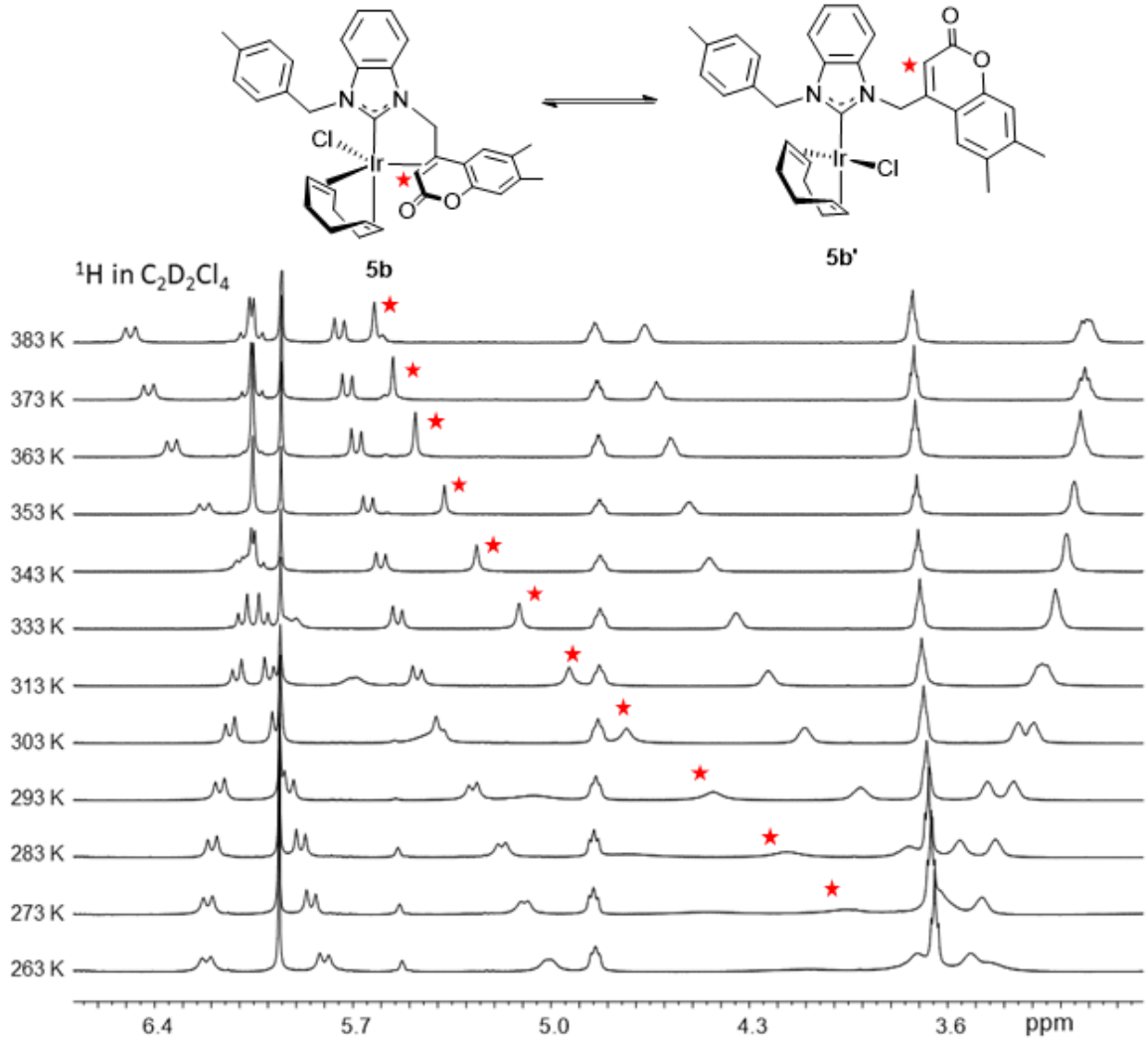

Figure S4. Stacked ^{1}H NMR spectra of **5b⇌5b'** in $C_2D_2Cl_4$ at different temperatures.

5. NMR spectra of coumarin-functionalized azolium salts and Ir-NHC complexes

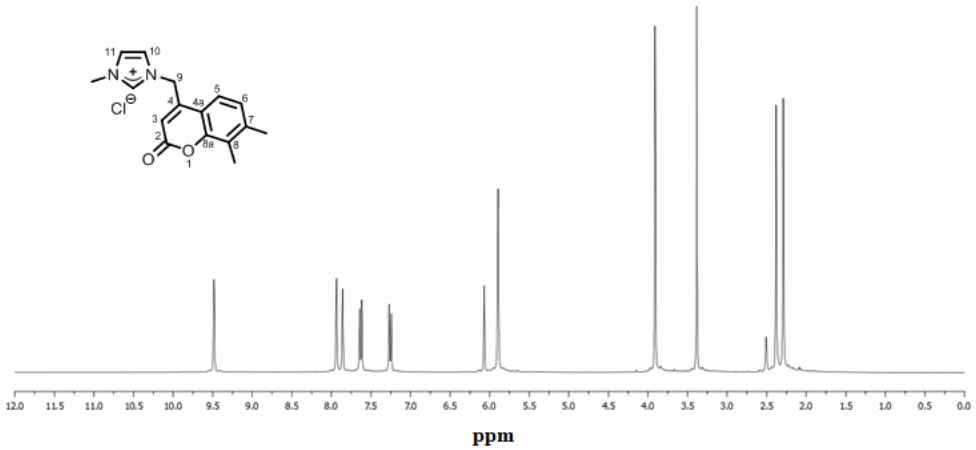

Figure S5. ^{1}H NMR spectrum of **2a** in DMSO-d_6 at 298 K.

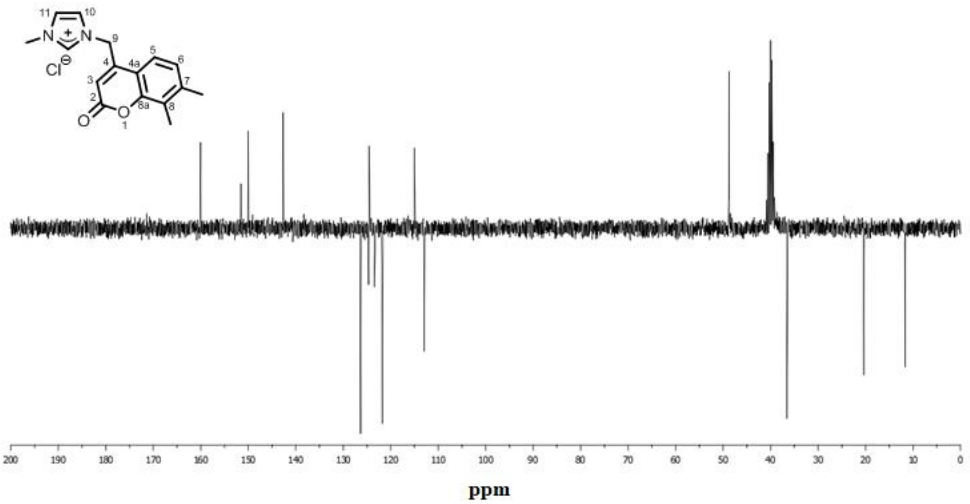

Figure S6. $^{13}C\{^{1}H\}$-APT NMR spectrum of **2a** in DMSO-d_6 at 298 K.

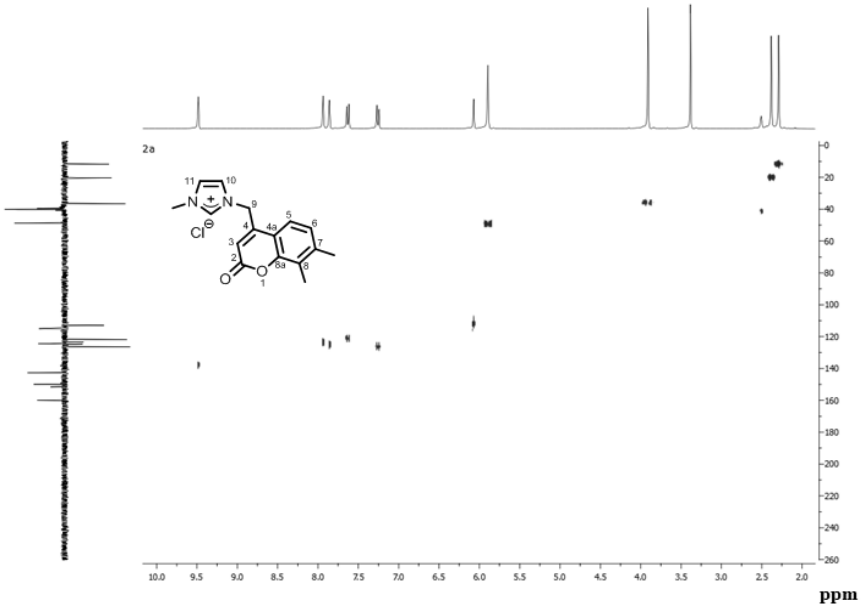

Figure S7. ^{13}C-^{1}H HSQC spectrum of **2a** in DMSO-d_6 at 298 K.

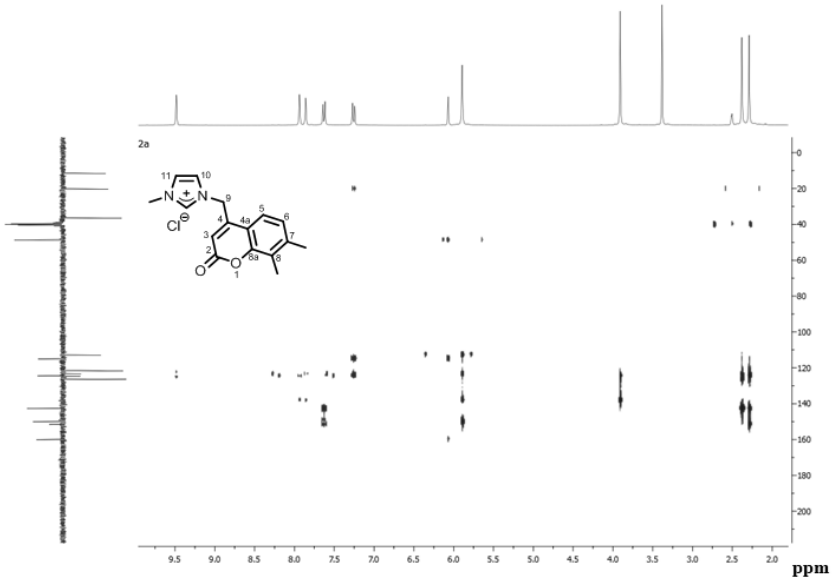

Figure S8. ^{13}C-^{1}H HMBC spectrum of **2a** in DMSO-d_6 at 298 K.

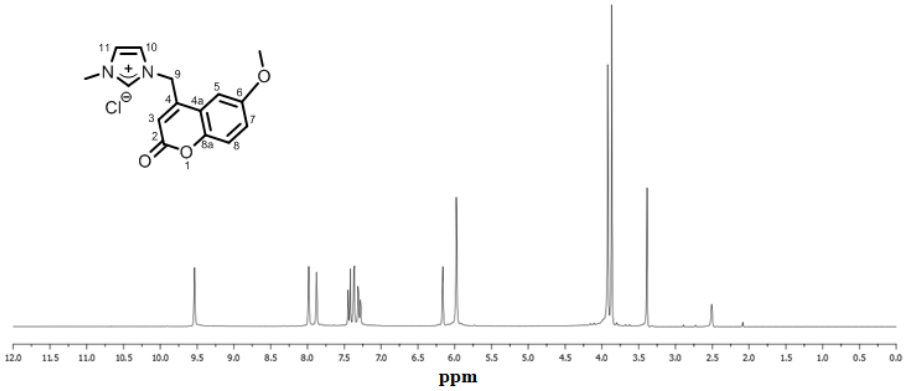

Figure S9. ^{1}H NMR spectrum of **2b** in DMSO-d_6 at 298 K.

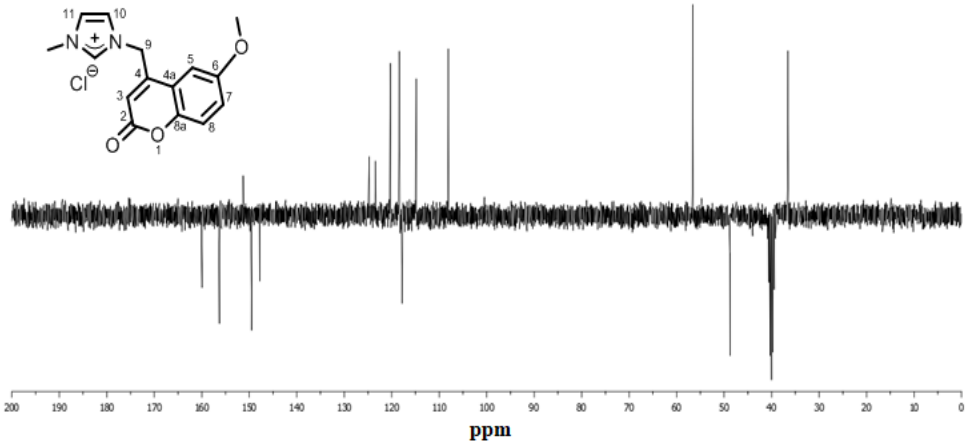

Figure S10. ^{13}C{^{1}H}-APT NMR spectrum of **2b** in DMSO-d_6 at 298 K.

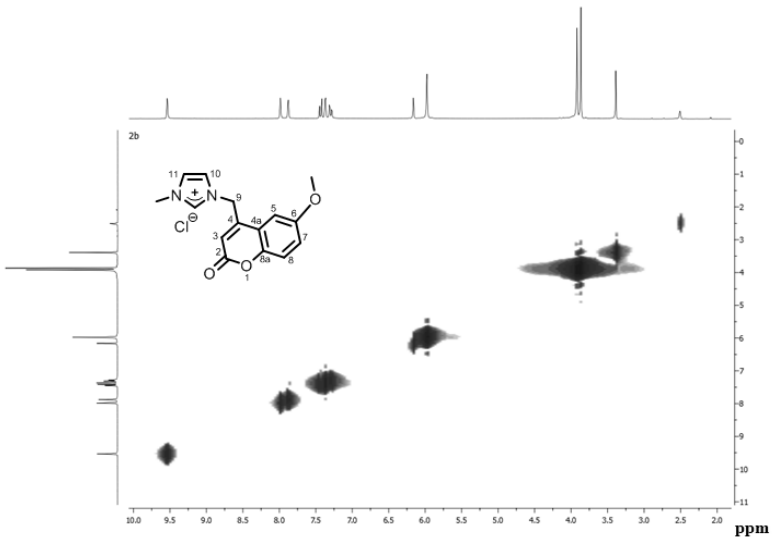

Figure S11. ^{1}H-^{1}H COSY spectrum of **2b** in DMSO-d_6 at 298 K.

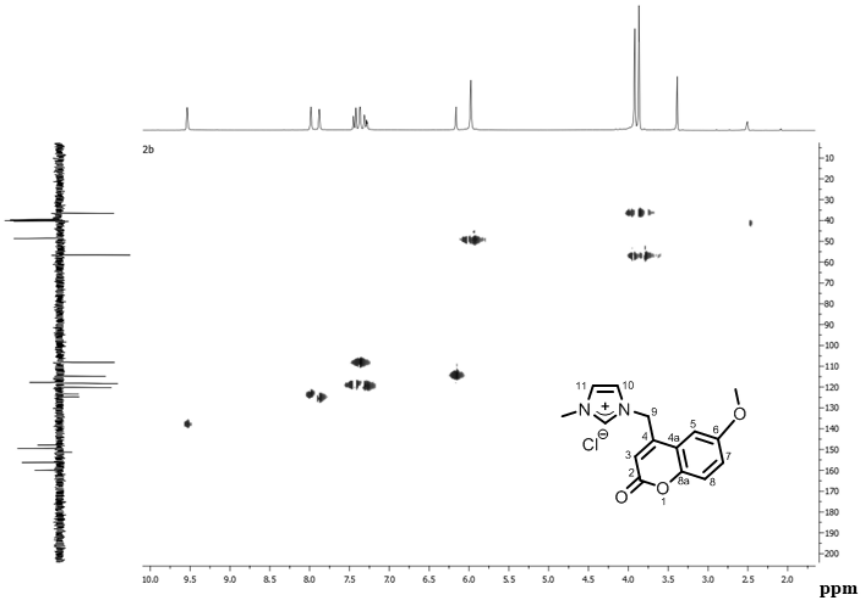

Figure S12. ^{13}C-^{1}H HSQC spectrum of **2b** in DMSO-d_6 at 298 K.

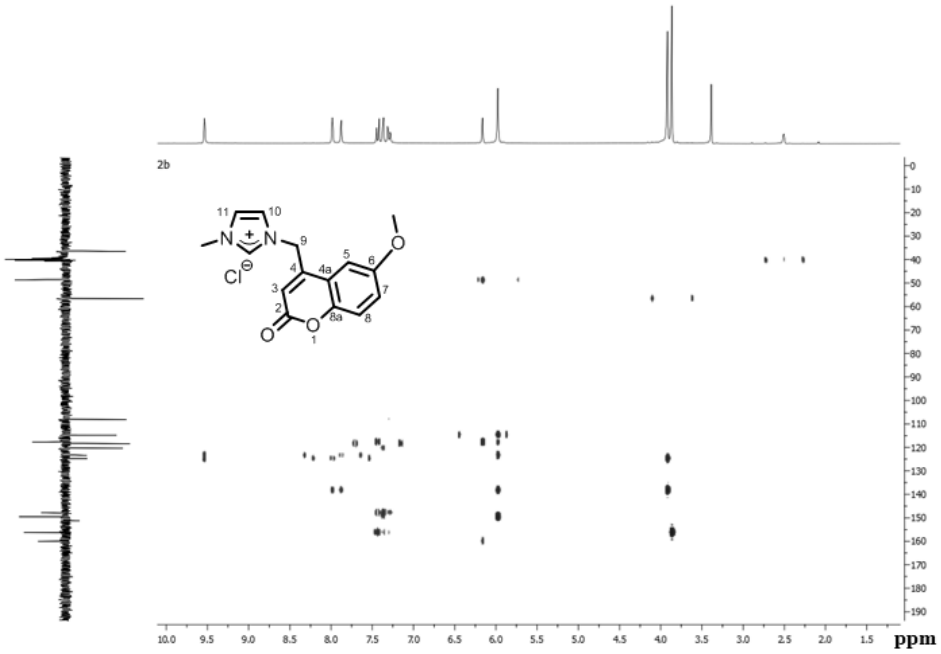

Figure S13. ^{13}C-^{1}H HMBC spectrum of **2b** in DMSO-d_6 at 298 K.

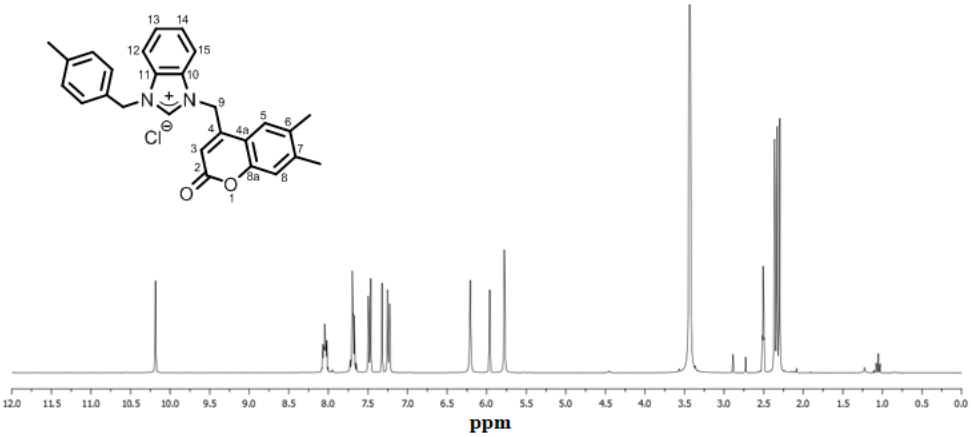

Figure S14. ^{1}H NMR spectrum of **3b** in DMSO-d_6 at 298 K.

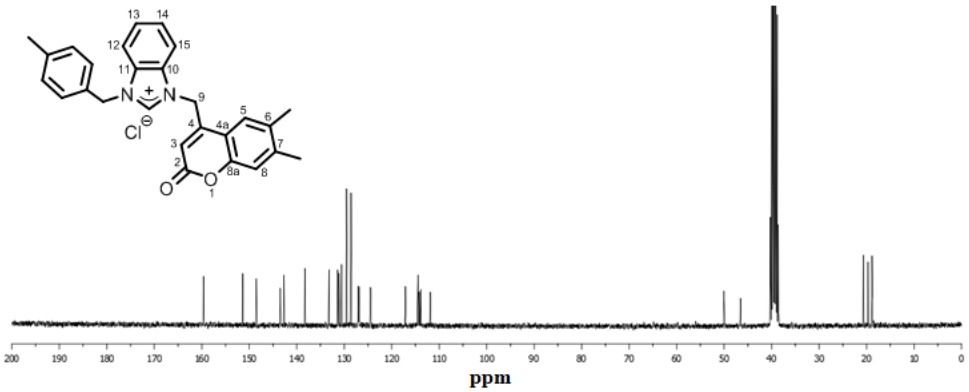

Figure S15. $^{13}C\{^{1}H\}$ NMR spectrum of **3b** in DMSO-d_6 at 298 K.

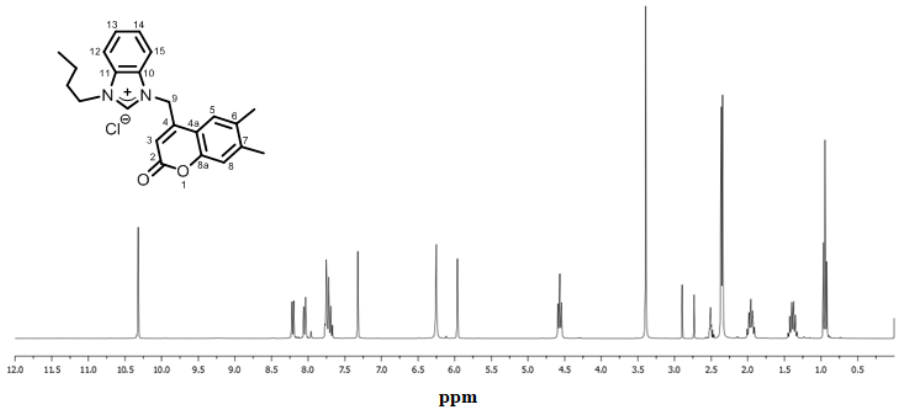

Figure S16. ^{1}H NMR spectrum of **3c** in DMSO-d_6 at 298 K.

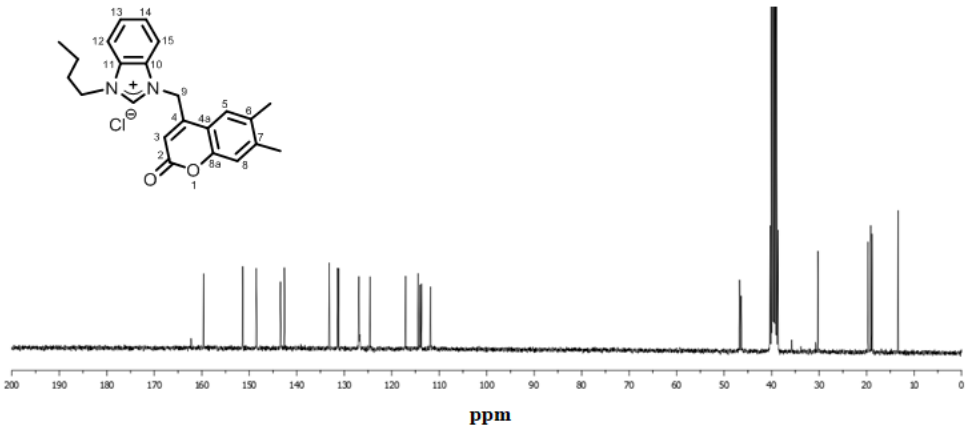

Figure S17. $^{13}C\{^{1}H\}$ NMR spectrum of **3c** in DMSO-d_6 at 298 K.

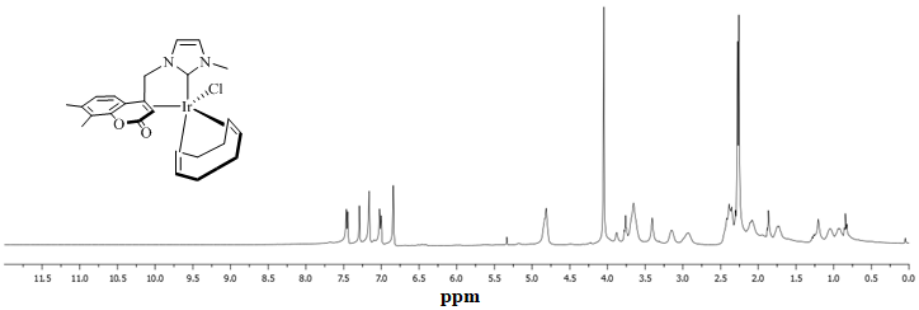

Figure S18. ^{1}H NMR spectrum of **4a** in $CDCl_3$ at 213 K.

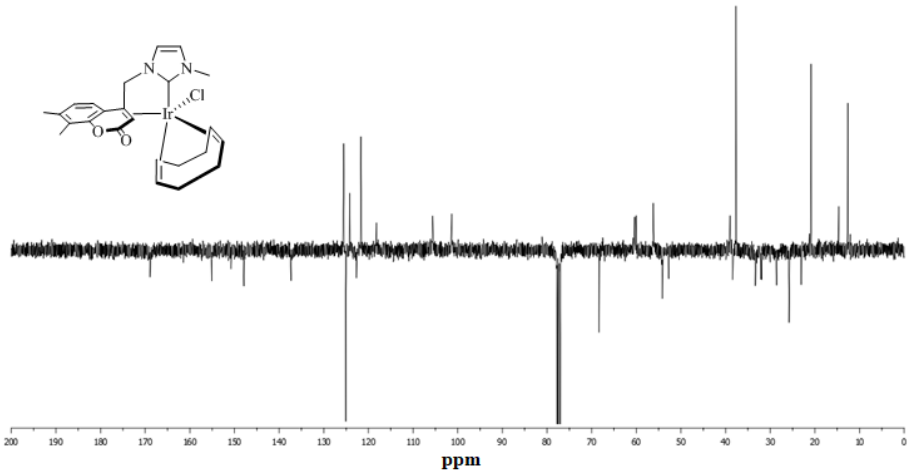

Figure S19. $^{13}C\{^{1}H\}$-APT NMR spectrum of **4a** in $CDCl_3$ at 213 K.

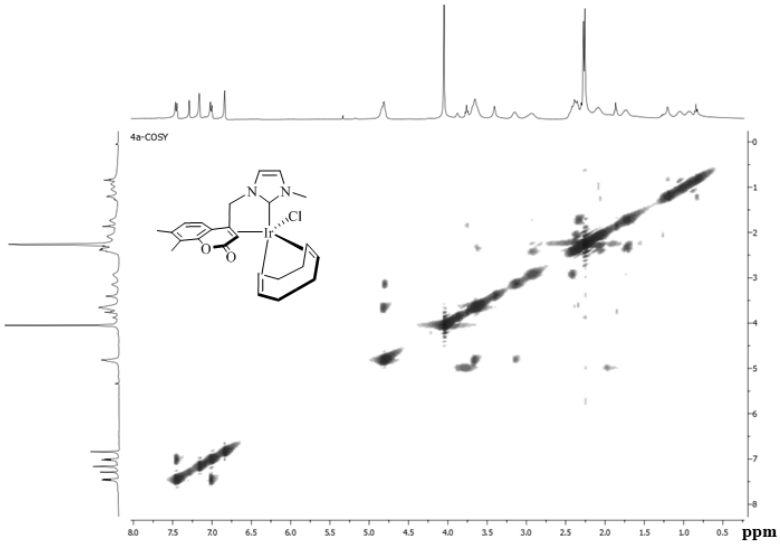

Figure S20. ^{1}H-^{1}H COSY spectrum of **4a** in $CDCl_3$ at 213 K.

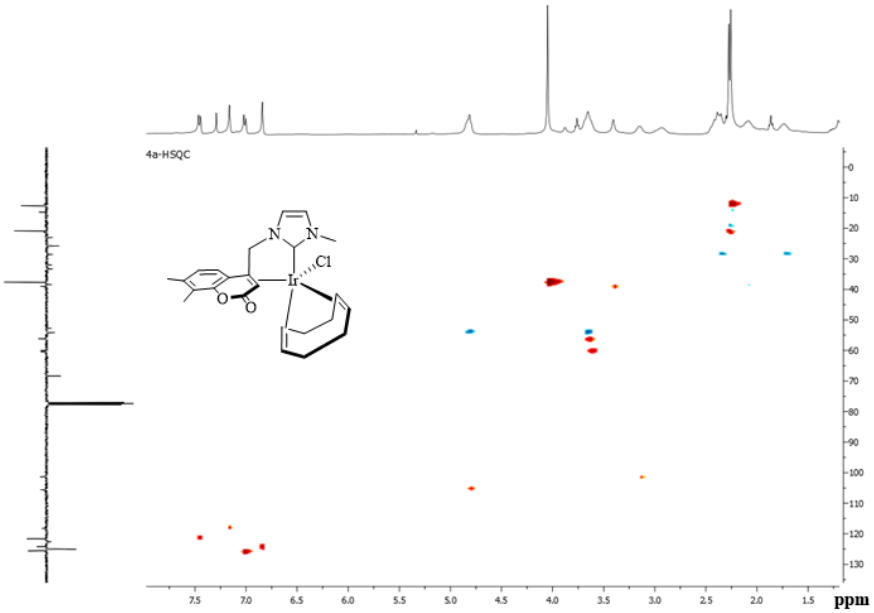

Figure S21. ^{13}C-^{1}H HSQC spectrum of **4a** in $CDCl_3$ at 213 K.

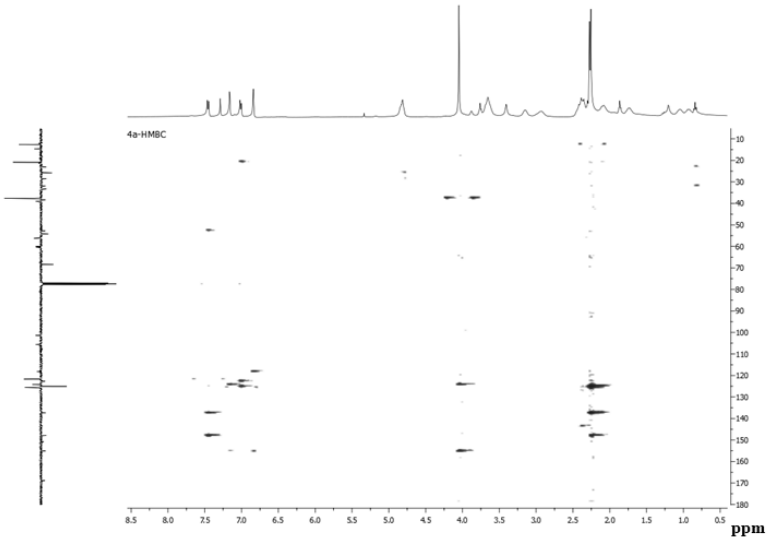

Figure S22. ^{13}C-^{1}H HMBC spectrum of **4a** in $CDCl_3$ at 213 K.

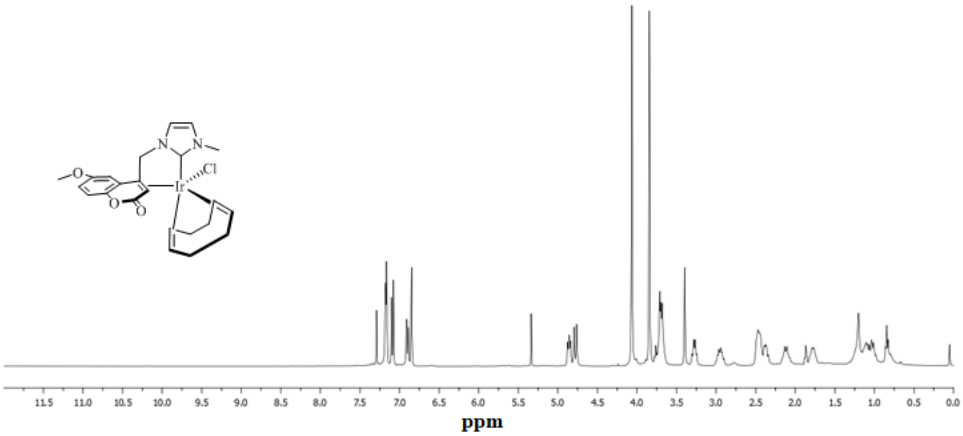

Figure S23. ^{1}H NMR spectrum of **4b** in $CDCl_3$ at 213 K.

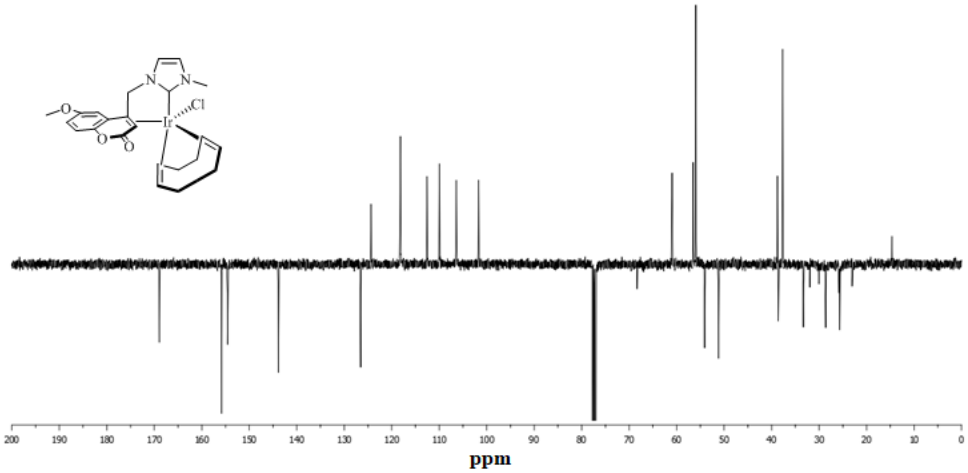

Figure S24. $^{13}C\{^{1}H\}$-APT NMR spectrum of **4b** in $CDCl_3$ at 213 K.

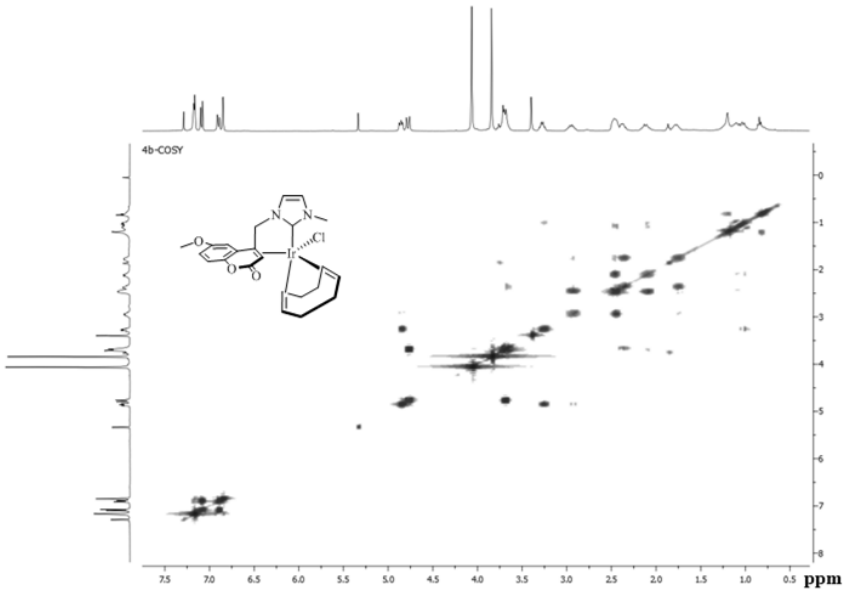

Figure S25. ^{1}H-^{1}H COSY spectrum of **4b** in $CDCl_3$ at 213 K.

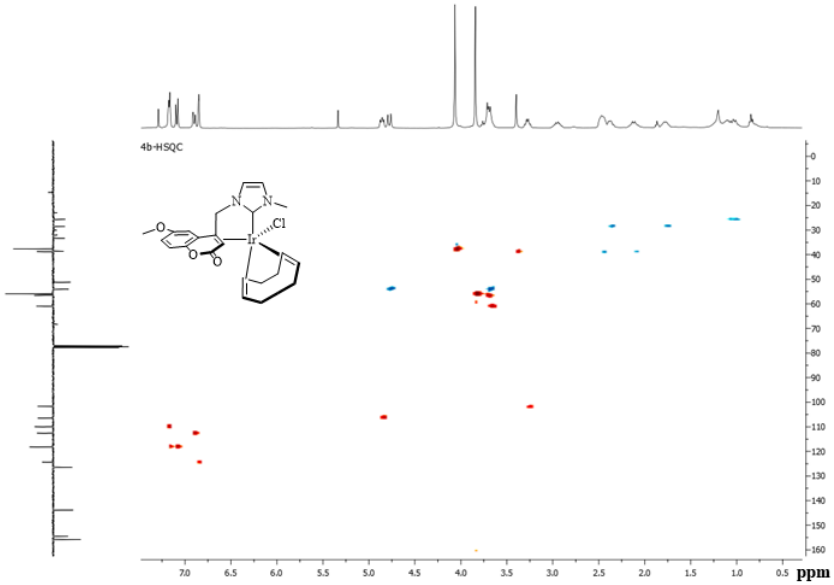

Figure S26. ^{13}C-^{1}H HSQC spectrum of **4b** in $CDCl_3$ at 213 K.

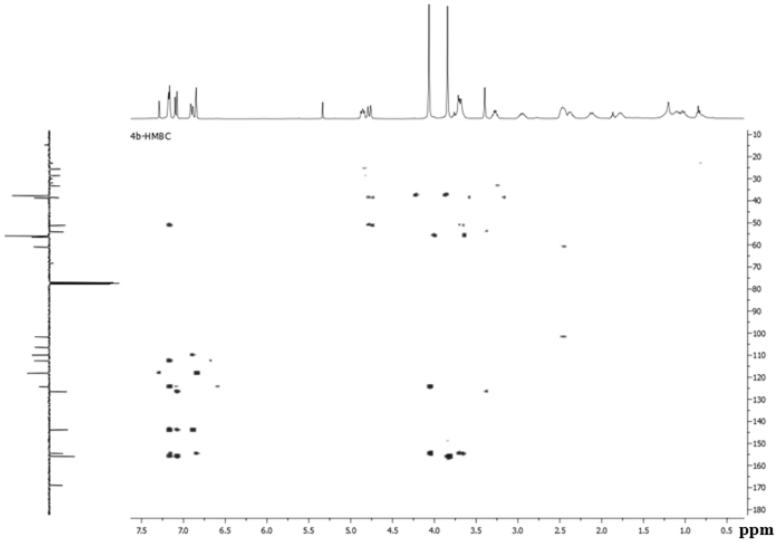

Figure S27. ^{13}C-^{1}H HMBC spectrum of **4b** in $CDCl_3$ at 213 K.

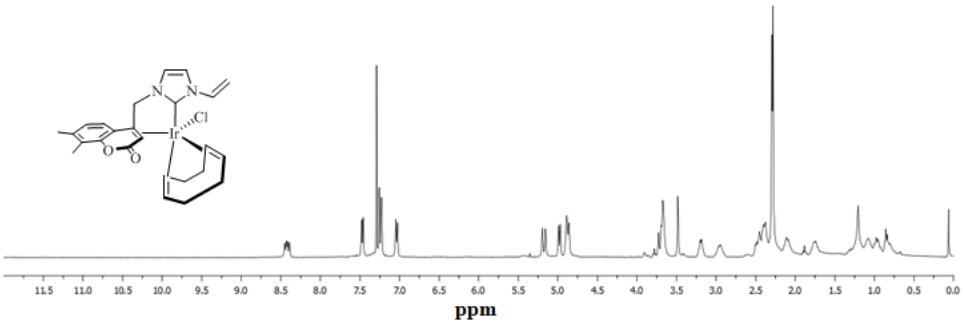

Figure S28. ^{1}H NMR spectrum of **4c** in $CDCl_3$ at 213 K.

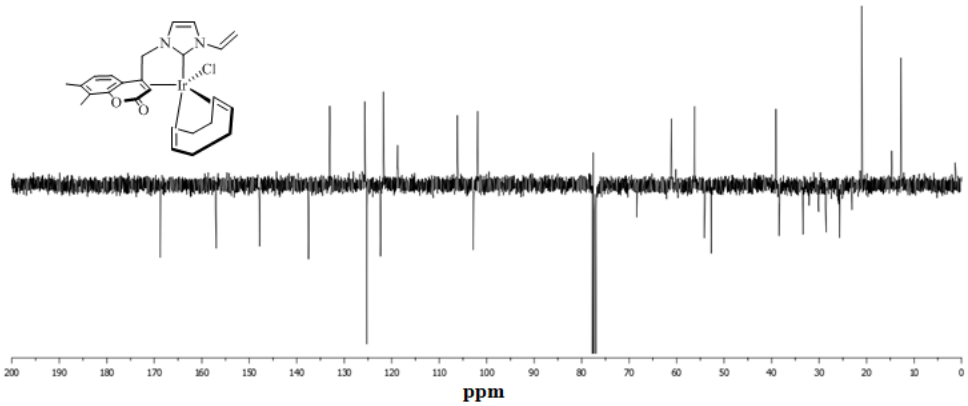

Figure S29. $^{13}C\{^{1}H\}$-APT NMR spectrum of **4c** in $CDCl_3$ at 213 K.

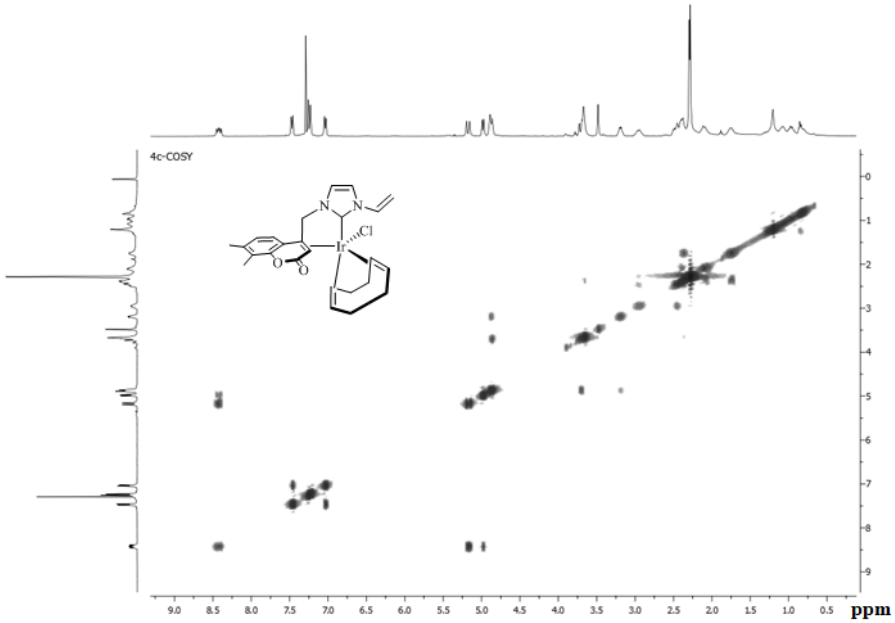

Figure S30. ^{1}H-^{1}H COSY spectrum of **4c** in $CDCl_3$ at 213 K.

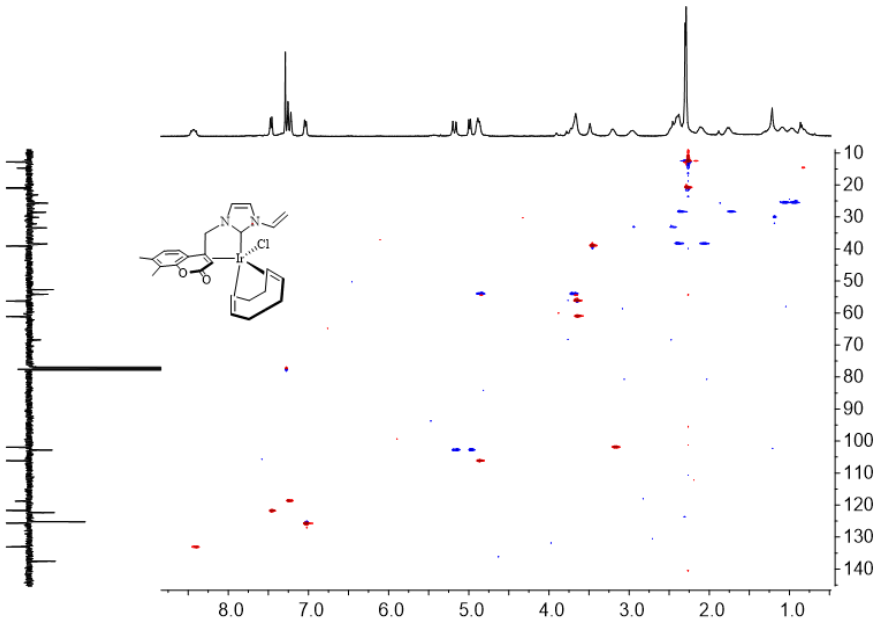

Figure S31. ^{13}C-^{1}H HSQC spectrum of **4c** in $CDCl_3$ at 213 K.

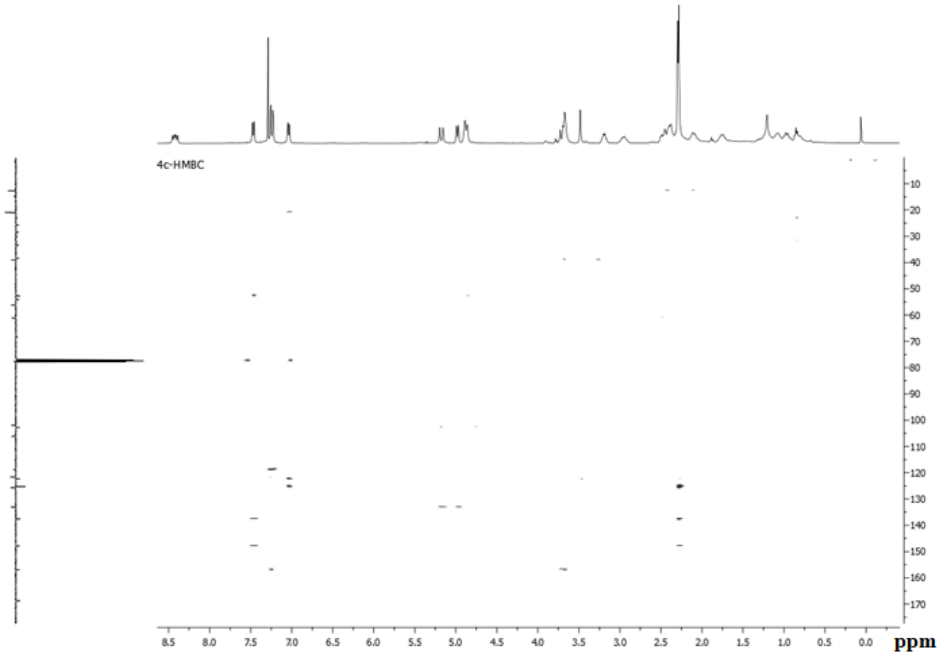

Figure S32. ^{13}C-^{1}H HMBC spectrum of **4c** in $CDCl_3$ at 213 K.

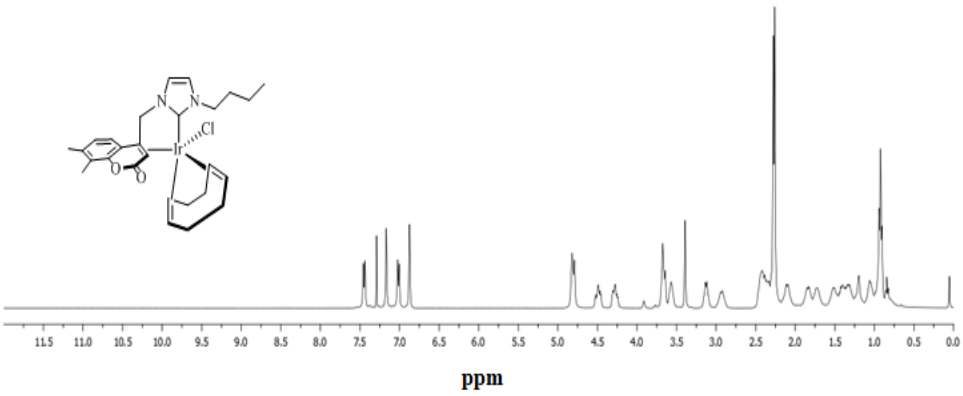

Figure S33. ^{1}H NMR spectrum of **4d** in $CDCl_3$ at 213 K.

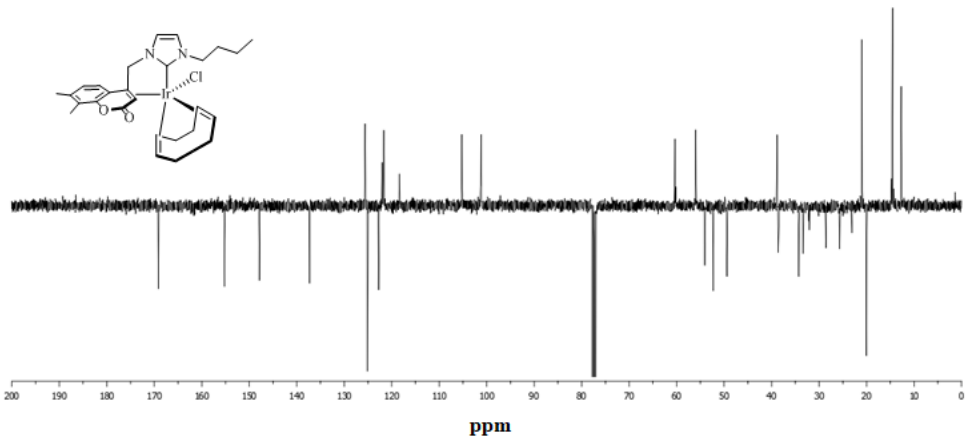

Figure S34. $^{13}C\{^{1}H\}$-APT NMR spectrum of **4d** in $CDCl_3$ at 213 K.

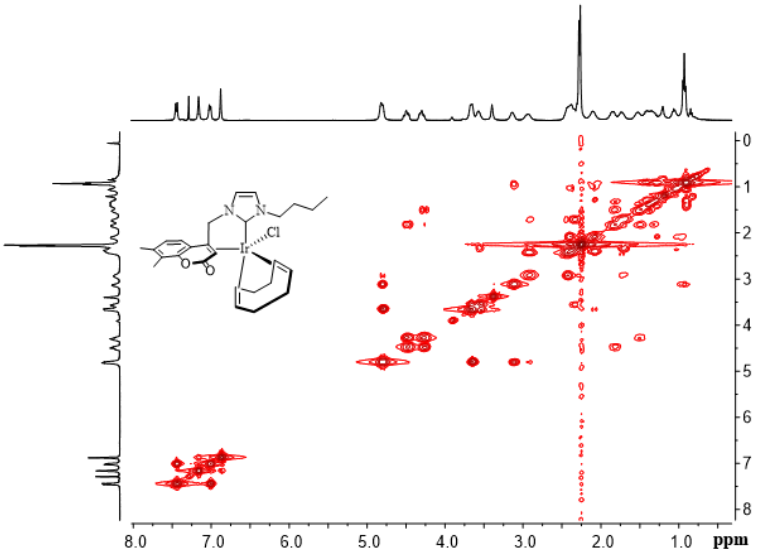

Figure S35. ^{1}H-^{1}H COSY spectrum of **4d** in $CDCl_3$ at 213 K.

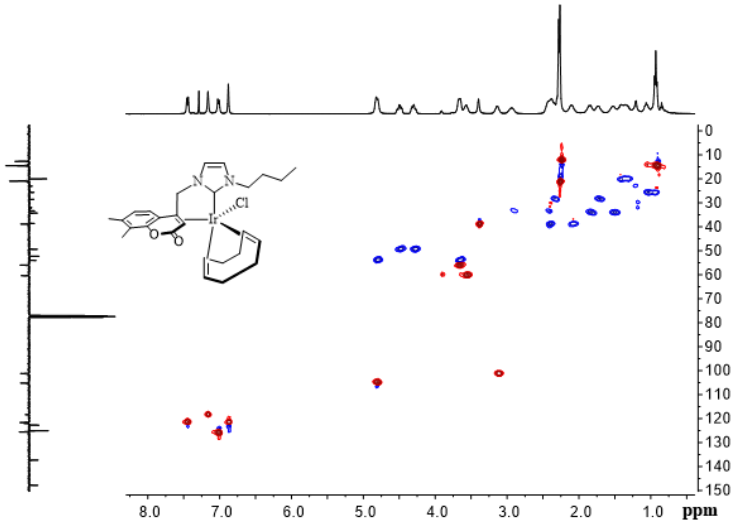

Figure S36. ^{13}C-^{1}H HSQC spectrum of **4d** in $CDCl_3$ at 213 K.

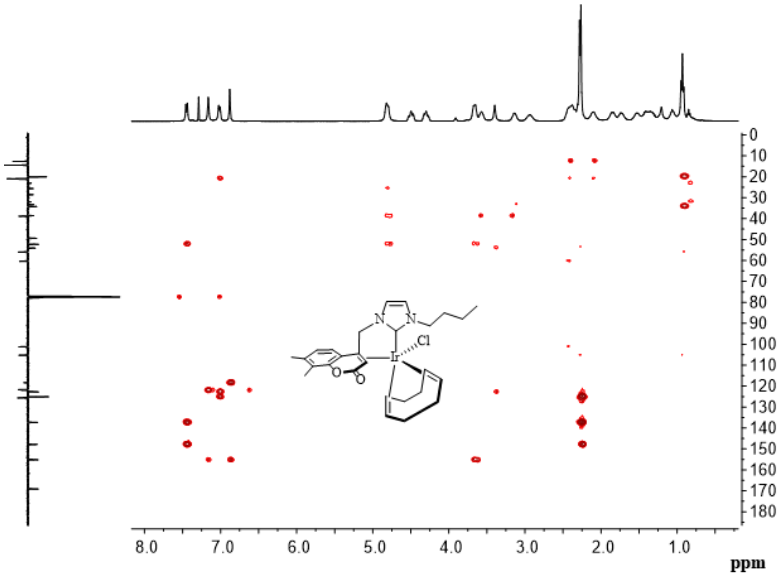

Figure S37. ^{13}C-^{1}H HMBC spectrum of **4d** in $CDCl_3$ at 213 K.

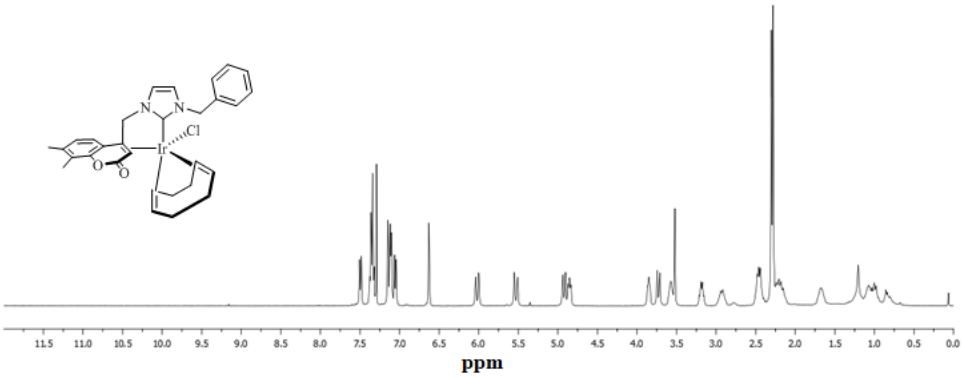

Figure S38. ^{1}H NMR spectrum of **4e** in $CDCl_3$ at 213 K.

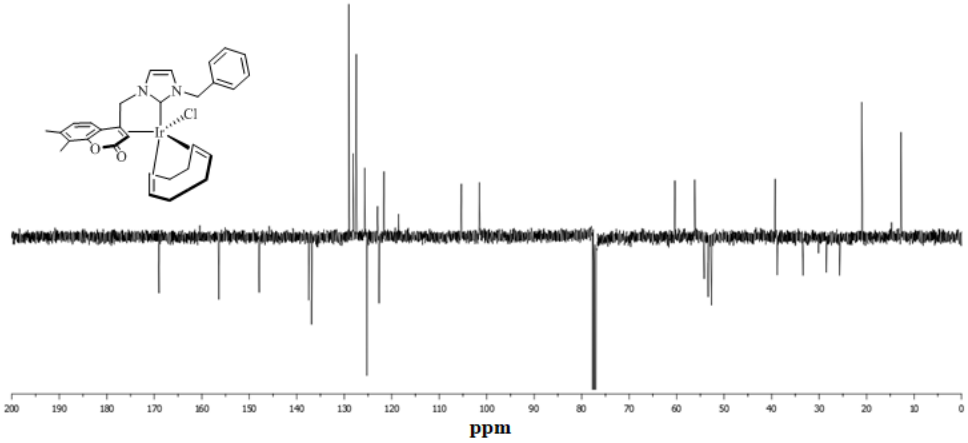

Figure S39. $^{13}C\{^{1}H\}$-APT NMR spectrum of **4e** in $CDCl_3$ at 213 K.

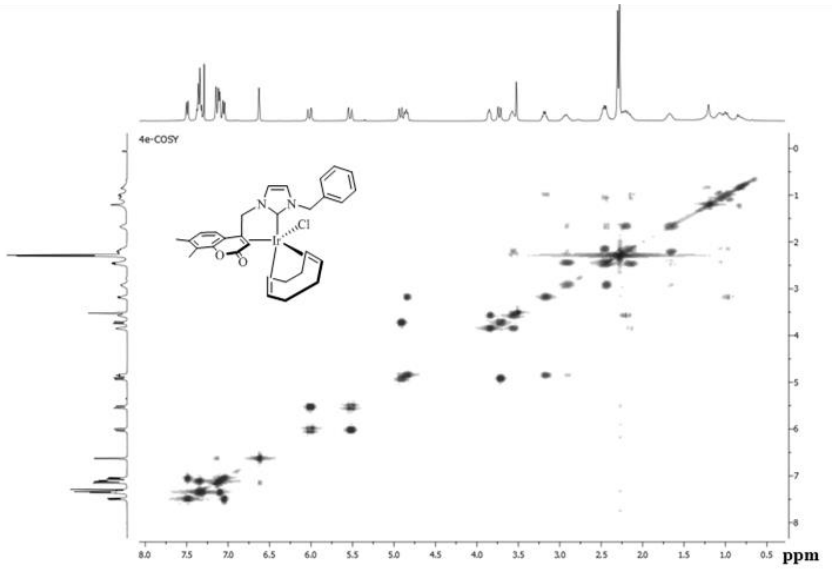

Figure S40. ^{1}H-^{1}H COSY spectrum of **4e** in $CDCl_3$ at 213 K.

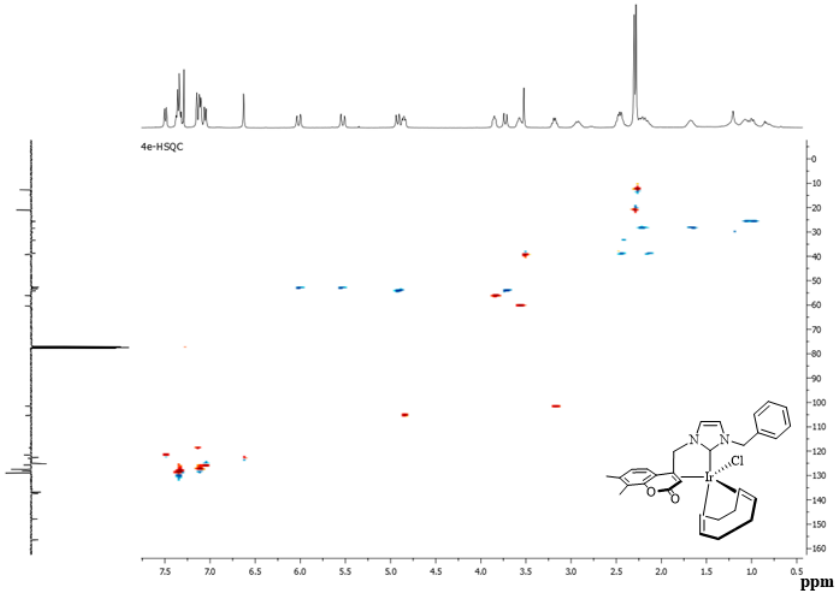

Figure S41. ^{13}C-^{1}H HSQC spectrum of **4e** in $CDCl_3$ at 213 K.

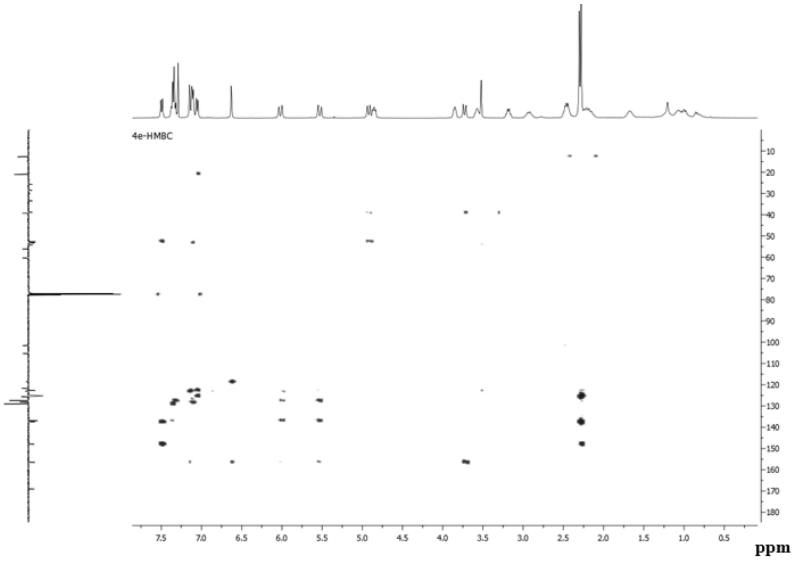

Figure S42. ^{13}C-^{1}H HMBC spectrum of **4e** in $CDCl_3$ at 213 K.

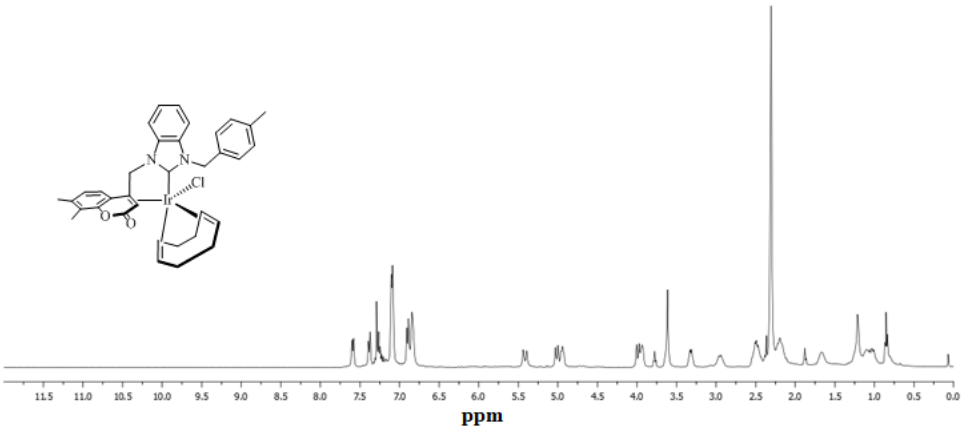

Figure S43. ^{1}H NMR spectrum of **5a** in $CDCl_3$ at 213 K.

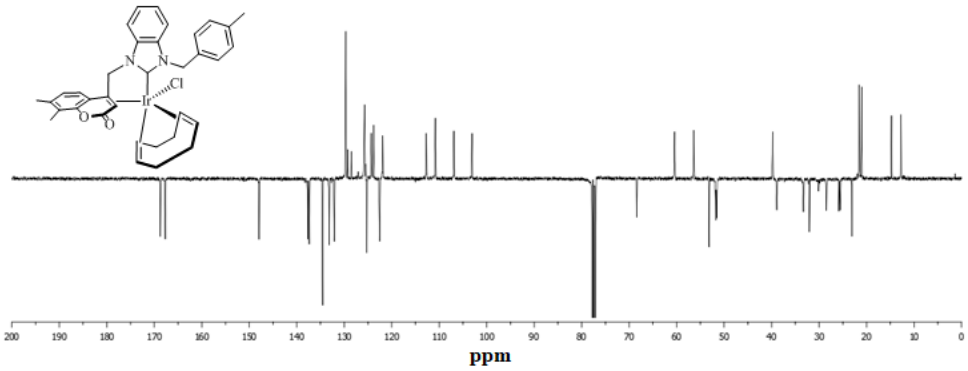

Figure S44. $^{13}C\{^{1}H\}$-APT NMR spectrum of **5a** in $CDCl_3$ at 213 K.

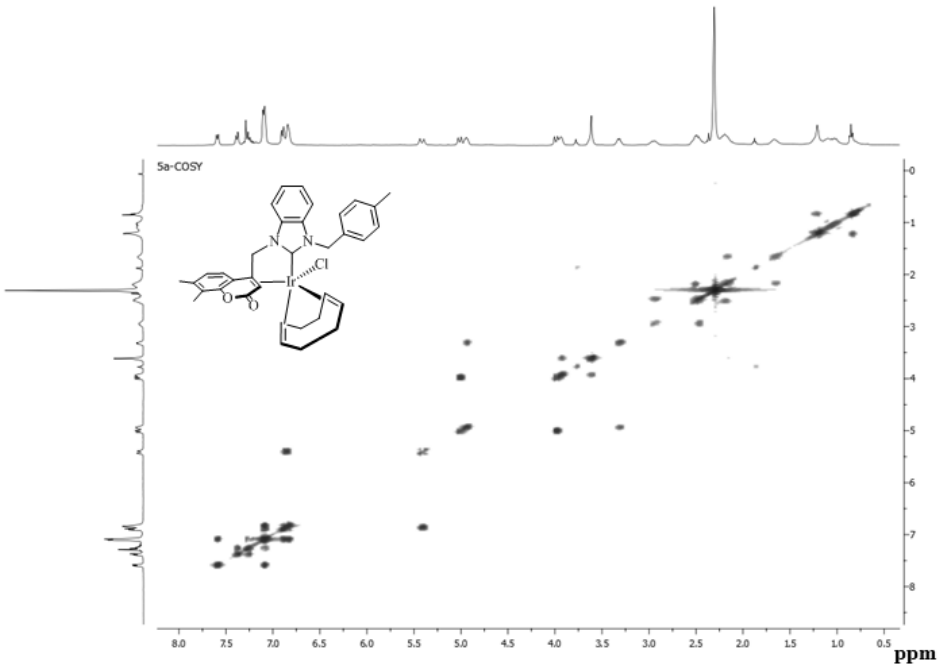

Figure S45. ^{1}H-^{1}H COSY spectrum of **5a** in $CDCl_3$ at 213 K.

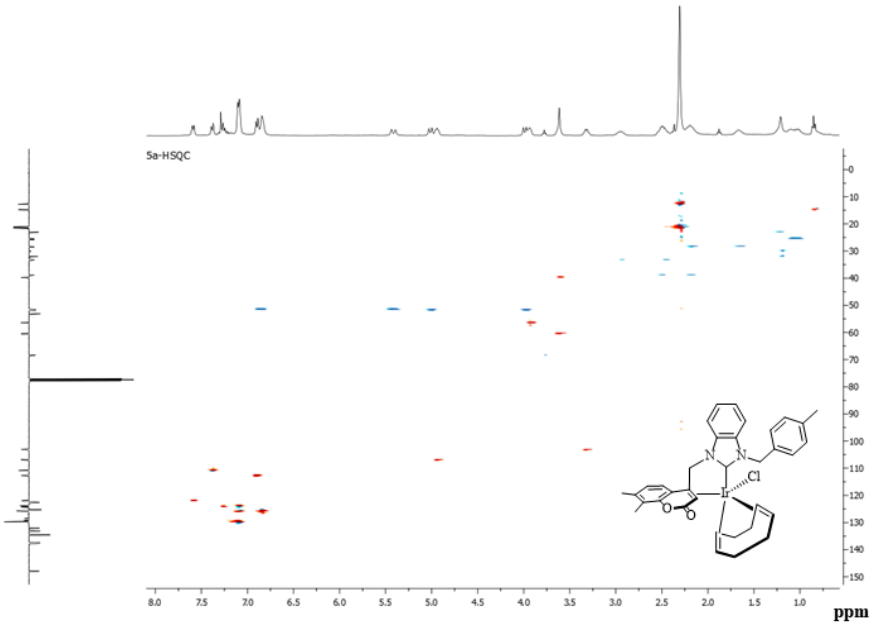

Figure S46. ^{13}C-^{1}H HSQC spectrum of **5a** in $CDCl_3$ at 213 K.

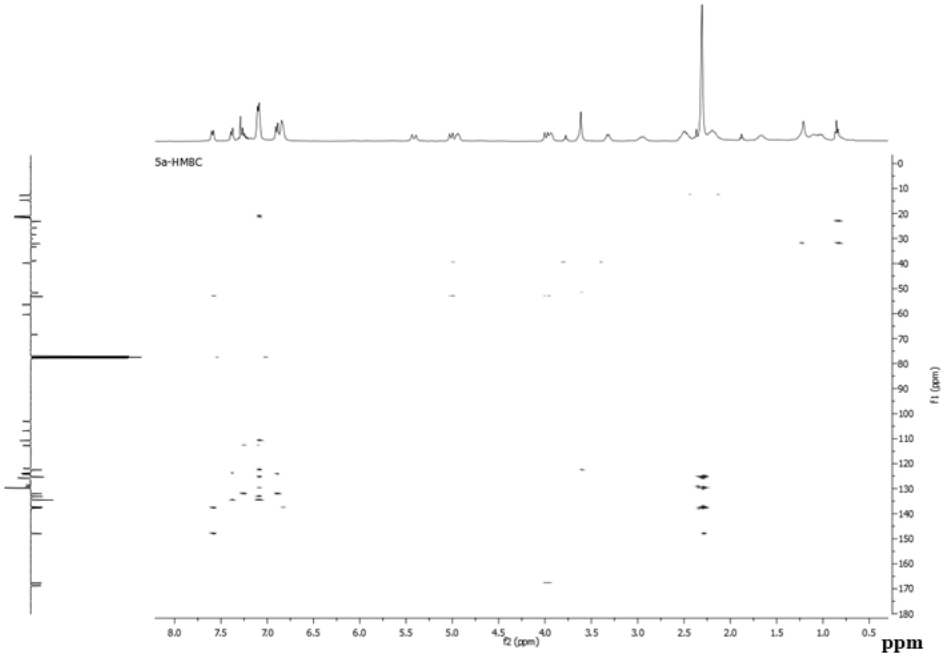

Figure S47. ^{13}C-^{1}H HMBC spectrum of **5a** in $CDCl_3$ at 213 K.

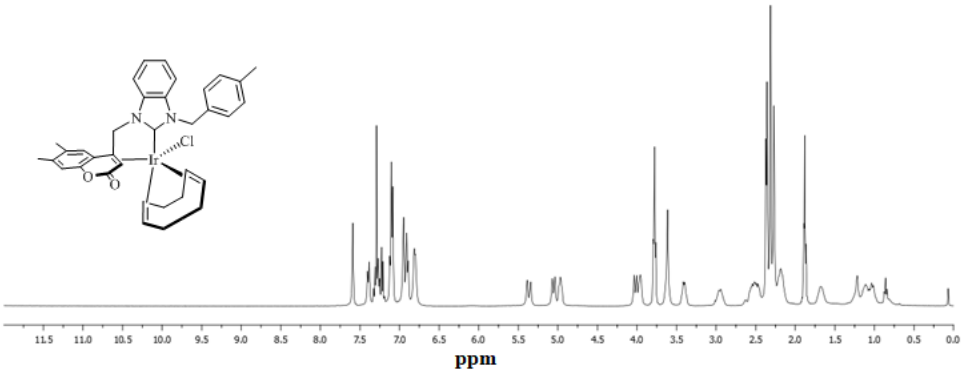

Figure S48. ^{1}H NMR spectrum of **5b** in $CDCl_3$ at 213 K.

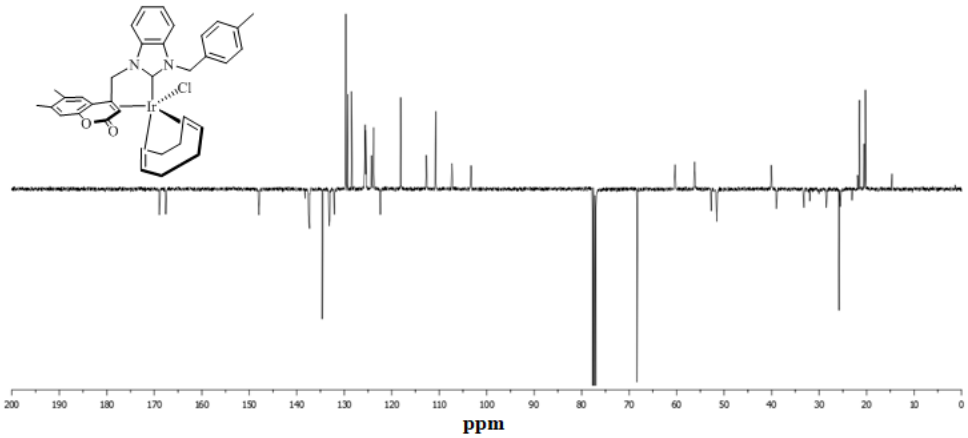

Figure S49. $^{13}C\{^{1}H\}$-APT NMR spectrum of **5b** in $CDCl_3$ at 213 K.

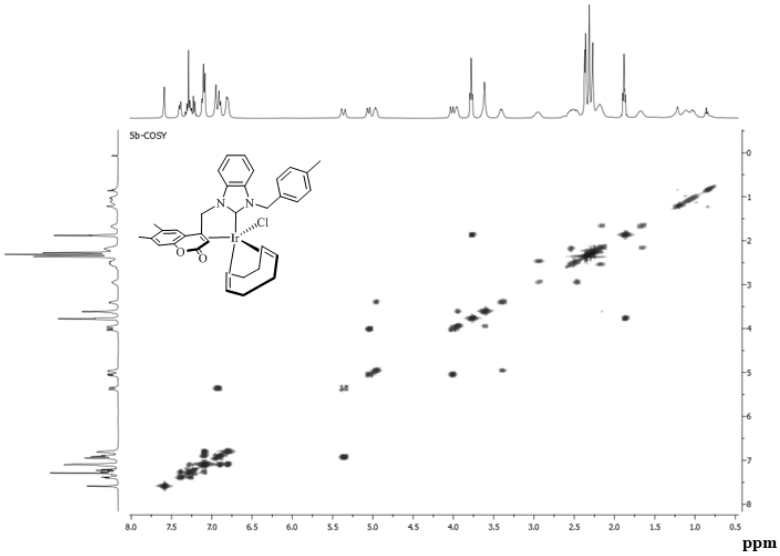

Figure S50. ^{1}H-^{1}H COSY spectrum of **5b** in $CDCl_3$ at 213 K.

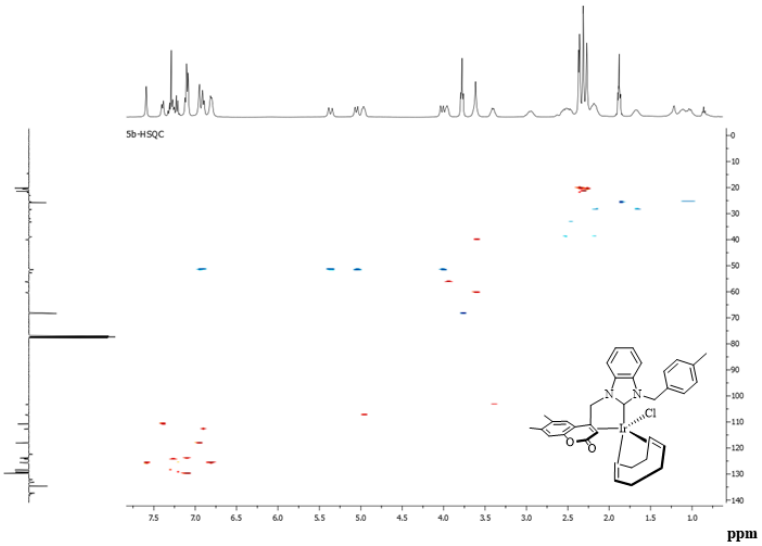

Figure S51. ^{13}C-^{1}H HSQC spectrum of **5b** in $CDCl_3$ at 213 K.

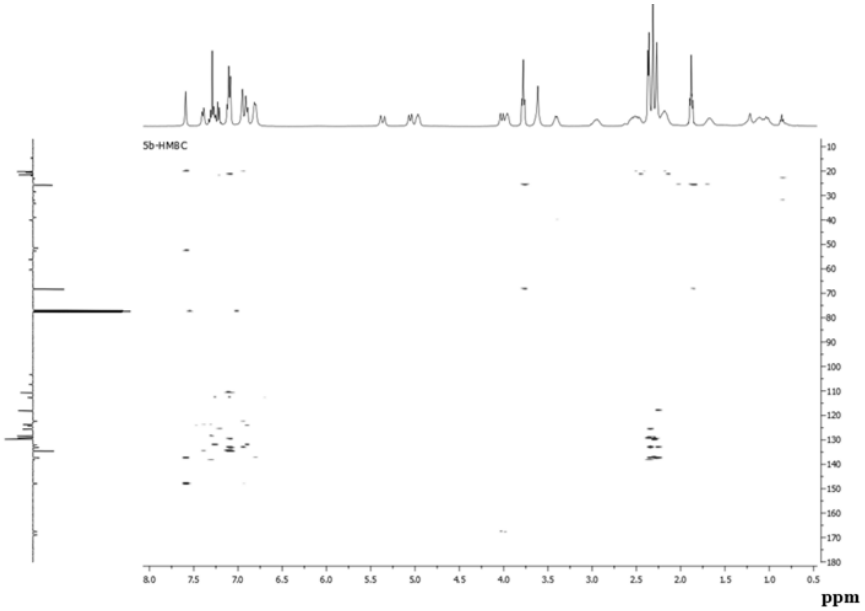

Figure S52. ^{13}C-^{1}H HMBC spectrum of **5b** in $CDCl_3$ at 213 K.

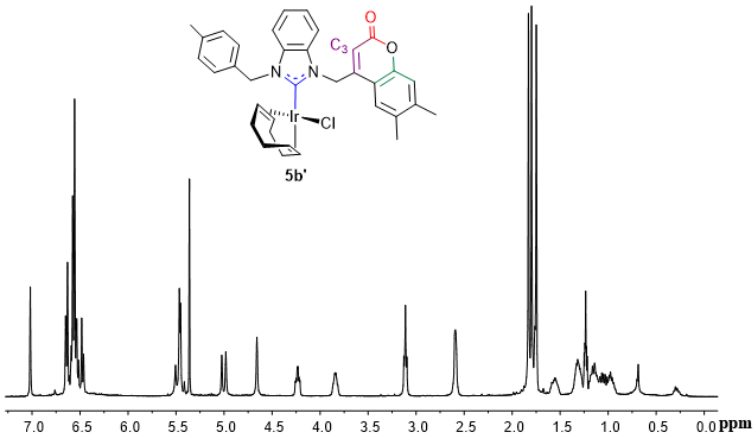

Figure S53. ^{1}H NMR spectrum of **5b'** in $C_2D_2Cl_4$ at 363 K.

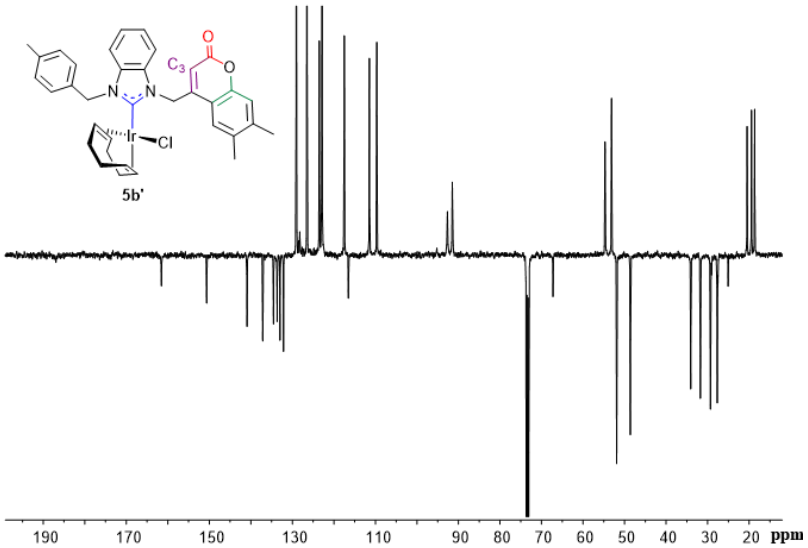

Figure S54. $^{13}C\{^{1}H\}$-APT NMR spectrum of **5b'** in $C_2D_2Cl_4$ at 363 K.

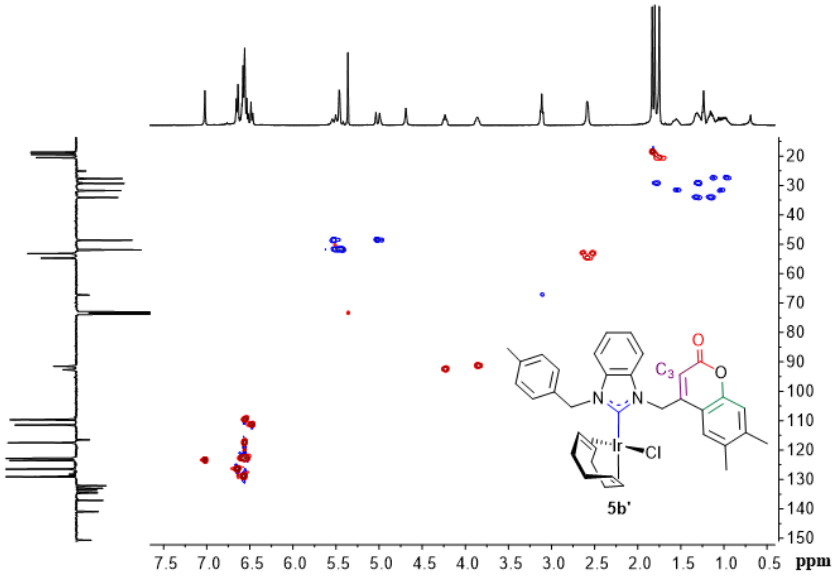

Figure S55. ^{13}C-^{1}H HSQC spectrum of **5b'** in $C_2D_2Cl_4$ at 363 K.

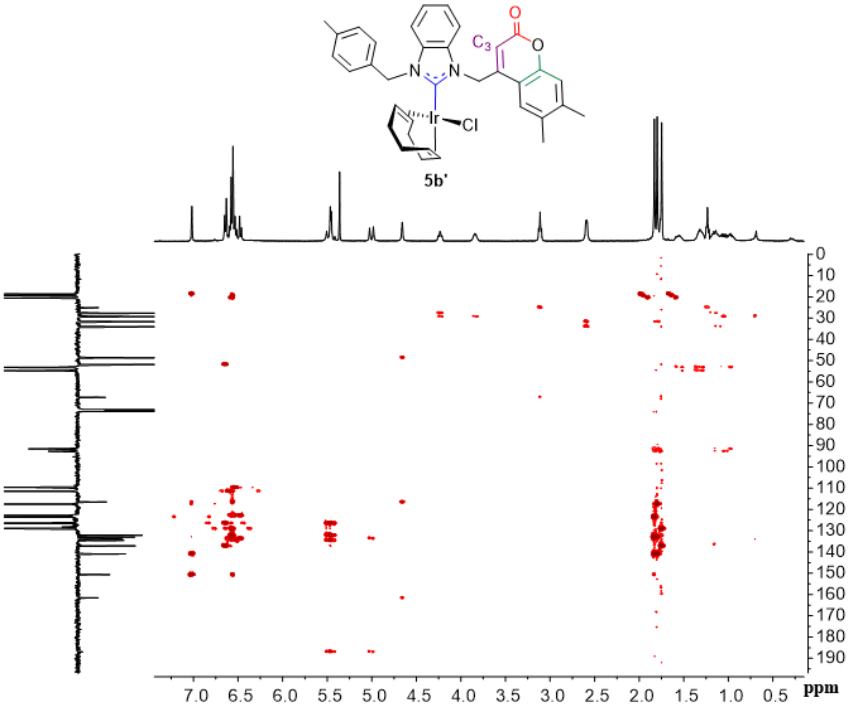

Figure S56. ^{13}C-^{1}H HMBC spectrum of **5b'** in $C_2D_2Cl_4$ at 363 K.

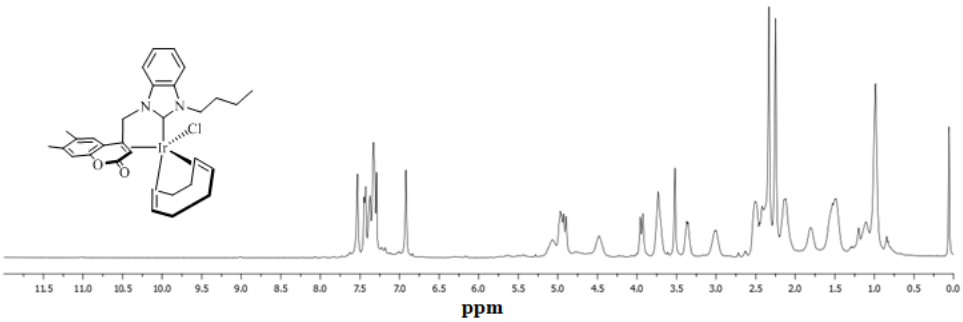

Figure S57. ^{1}H NMR spectrum of **5c** in $CDCl_3$ at 213 K.

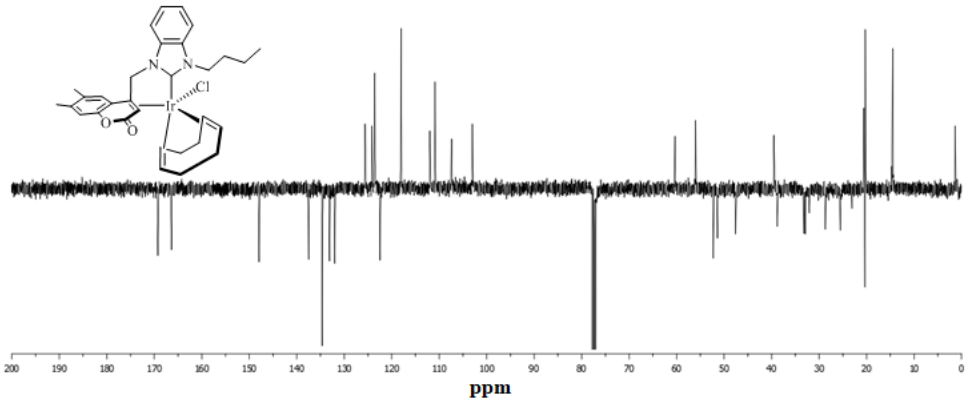

Figure S58. $^{13}C\{^{1}H\}$-APT NMR spectrum of **5c** in $CDCl_3$ at 213 K.

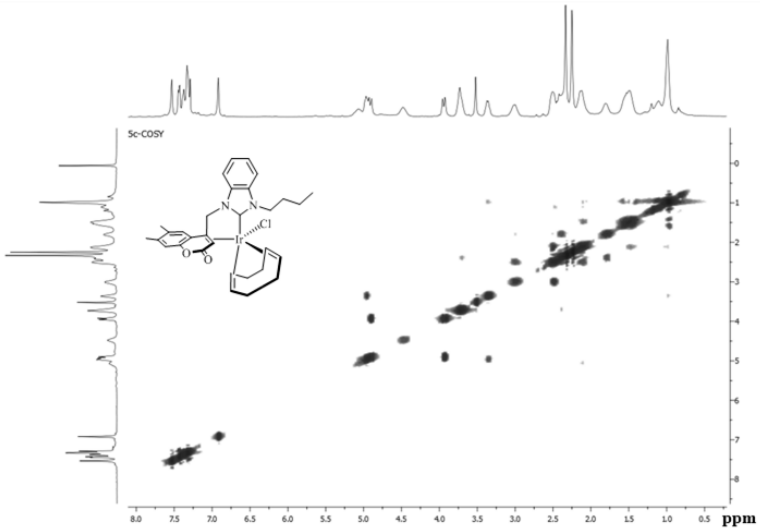

Figure S59. ^{1}H-^{1}H COSY spectrum of **5c** in $CDCl_3$ at 213 K.

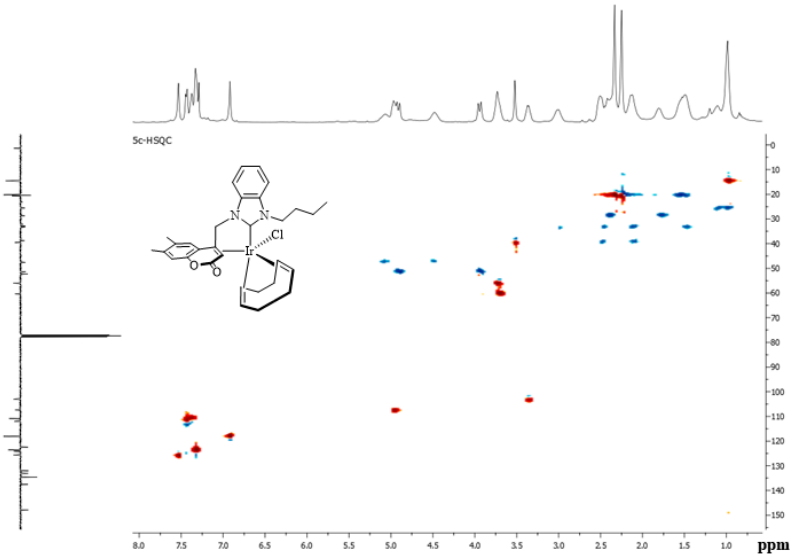

Figure S60. ^{13}C-^{1}H HSQC spectrum of **5c** in $CDCl_3$ at 213 K.

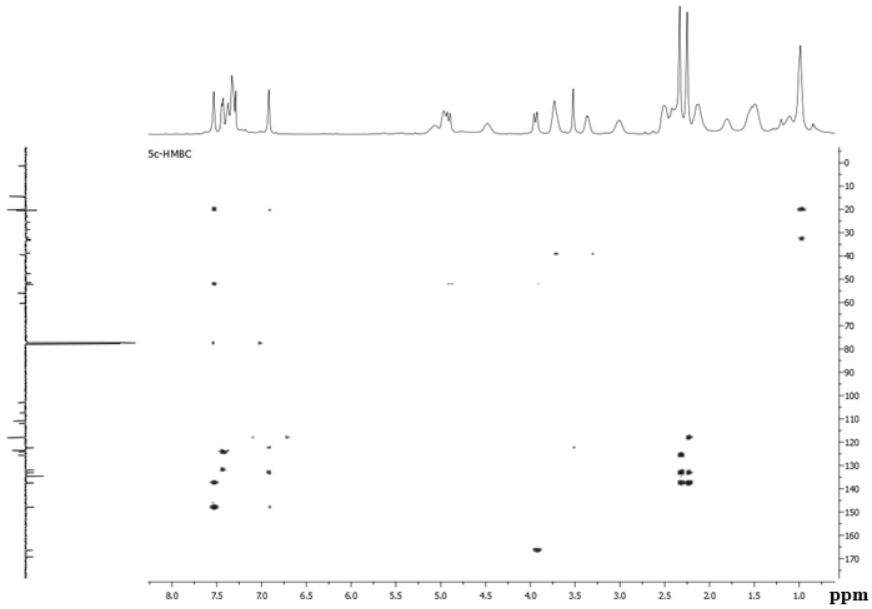

Figure S61. ^{13}C-^{1}H HMBC spectrum of **5c** in $CDCl_3$ at 213 K.

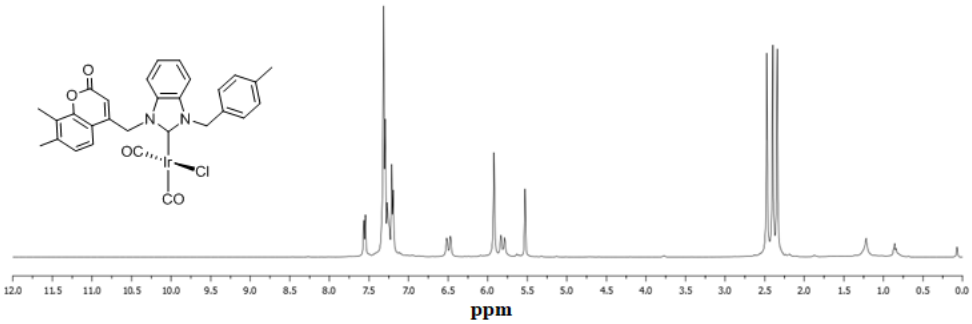

Figure S62. ^{1}H NMR spectrum of **6** in $CDCl_3$ at 213 K.

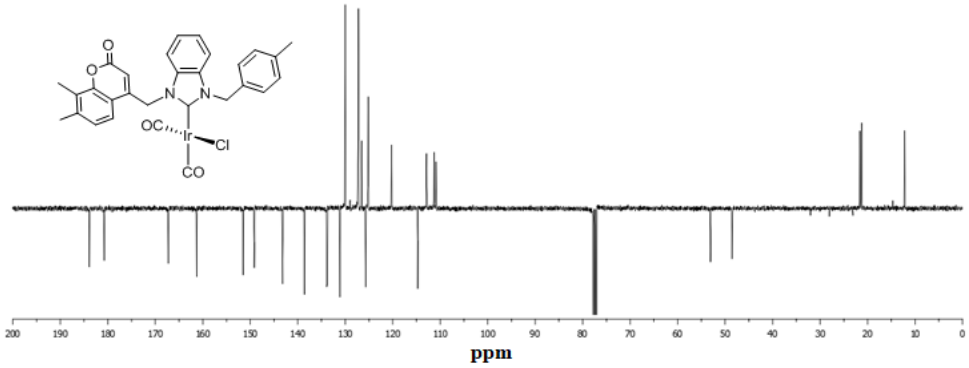

Figure S63. $^{13}C\{^{1}H\}$-APT NMR spectrum of **6** in $CDCl_3$ at 213 K.

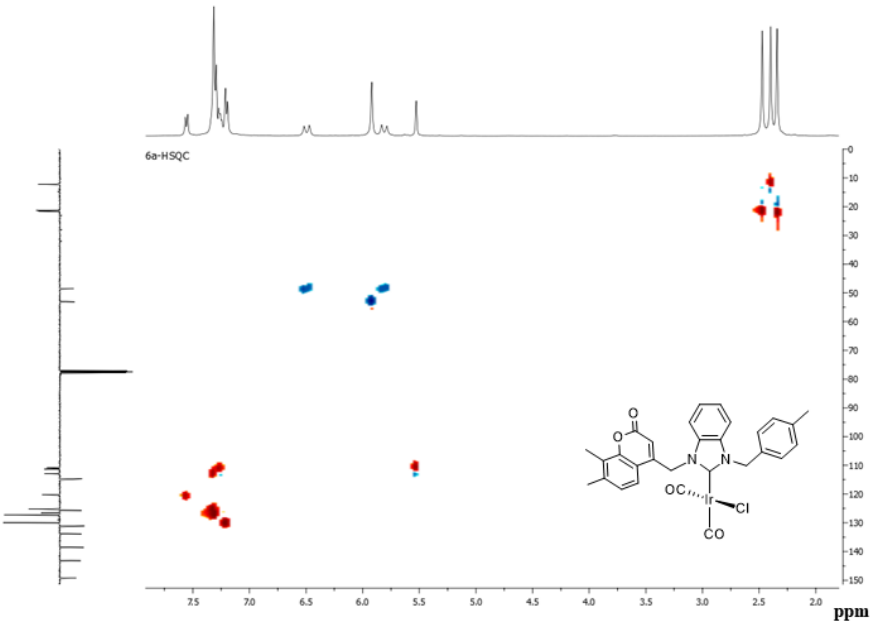

Figure S64. ^{13}C-^{1}H HSQC spectrum of **6** in $CDCl_3$ at 213 K.

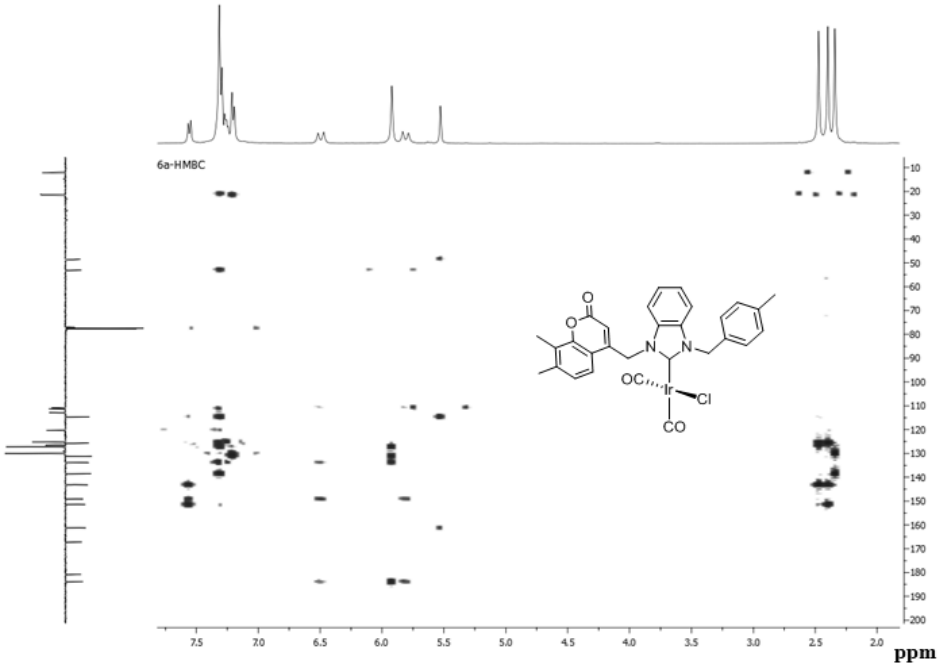

Figure S65. ^{13}C-^{1}H HMBC spectrum of **6** in $CDCl_3$ at 213 K.

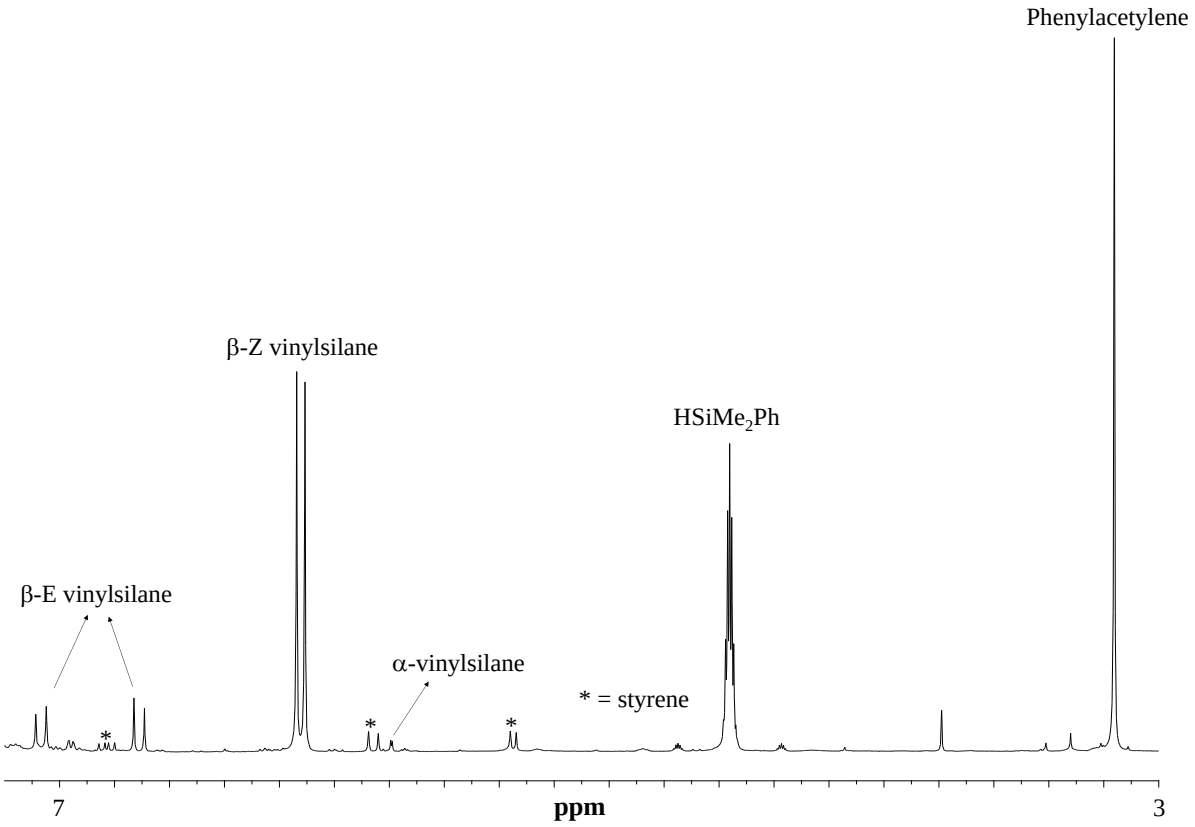

Figure S66. Representative ^{1}H NMR spectrum ($CDCl_3$) for the identification of hydrosilylation reaction products: hydrosilylation of phenylacetylene with $HSiMe_2Ph$ catalyzed by **6** after 24 h (entry 9, Table 1).

References

1 M. S. Frasinyuk, S. P. Bondarenko, V. P. Khilya, *Chem. Nat. Compd.*, 2006, **42**, 142-14.

2 M. O. Karataş, A. Di Giuseppe, V. Passarelli, B. Alıcı , J. J. Perez-Torrente, L. A. Oro, I. Özdemir, R. Castarlenas, *Organometallics*, 2018, **37**, 191-202.